



City Research Online

City, University of London Institutional Repository

Citation: Caldana, R. and Fusai, G. (2013). A general closed-form spread option pricing formula. *Journal of Banking & Finance*, 37(12), pp. 4893-4906. doi: 10.1016/j.jbankfin.2013.08.016

This is the accepted version of the paper.

This version of the publication may differ from the final published version.

Permanent repository link: <https://openaccess.city.ac.uk/id/eprint/5993/>

Link to published version: <http://dx.doi.org/10.1016/j.jbankfin.2013.08.016>

Copyright: City Research Online aims to make research outputs of City, University of London available to a wider audience. Copyright and Moral Rights remain with the author(s) and/or copyright holders. URLs from City Research Online may be freely distributed and linked to.

Reuse: Copies of full items can be used for personal research or study, educational, or not-for-profit purposes without prior permission or charge. Provided that the authors, title and full bibliographic details are credited, a hyperlink and/or URL is given for the original metadata page and the content is not changed in any way.

A general closed-form spread option pricing formula

Abstract

We propose a new accurate method for pricing European spread options by extending the lower bound approximation of [Bjerk sund and Stensland \(2011\)](#) beyond the classical Black–Scholes framework. This is possible via a procedure requiring a univariate Fourier inversion. In addition, we are also able to obtain a new tight upper bound. Our method provides also an exact closed form solution via Fourier inversion of the exchange option price, generalizing the [Margrabe \(1978\)](#) formula. The method is applicable to models in which the joint characteristic function of the underlying assets forming the spread is known analytically. We test the performance of these new pricing algorithms performing numerical experiments on different stochastic dynamic models.¹

Keywords: Spread option, exchange option, stochastic process, characteristic function, Fourier inversion, control variate.

JEL: C63, G13

1. Introduction

A spread option is a contract written on the price difference of two underlying assets whose values at time t are denoted by $S_1(t)$ and $S_2(t)$. We consider European-type options for which the buyer, on the option exercise date T , has the right to receive the spread $S_2(T) - S_1(T)$, by paying the option's strike price K .

Since spreads between indexes and financial variables are popular across different markets, options

¹Acknowledgement: We would like to thank Laura Ballotta, Rossella Agliardi, Marco Airoidi, Stewart Hodges, Ioannis Kyriakou, Andrea Roncoroni and an anonymous referee for providing valuable comments on earlier versions of the paper. The paper was presented at XIV Workshop on Quantitative Finance, Rimini, and to the XXXVII Amases Conference, Stresa. We thank all the participants for their helpful feedback.

written on these spreads are also popular. They are used to speculate, mitigate basis risk, and even evaluate real assets. For a detailed review of different spread option types we refer to [Carmona and Durrelman \(2003b\)](#). We mention here just a few examples to stress how their applicability is broader than pure option pricing.

- [Girma and Paulson \(1998, 1999\)](#) discuss the profitability of spread-based trading strategies in petroleum markets, exploiting the fact that the spread between WTI and Brent futures prices is stationary. Thus this spread can be used as an indicator for buy and sell trading strategy using technical trading rules or via econometric techniques.
- Spread options can be used to mitigate the adverse movements of several indexes. An example is the crack spread that reflects the cost of refining crude oil into petroleum products. A refinery's output varies according to the plant design, its crude slate, and its operational and maintenance program, which can be related to seasonal product demand and changing market conditions. Therefore refineries take positions in crack spread futures strategies according to their physical and operational requirements and hedge against price fluctuations to mitigate risk or secure a profit margin on the production output. A recent empirical analysis on the crack spread is that of [Dempster et al. \(2008\)](#) and [Duan and Pliska \(2004\)](#).
- Spread options are also relevant in investment valuation problems. For example, in the energy industry a power generation unit can be priced using a real options approach. The spark spread measures the difference between the costs of operating a gas-powered generation unit, determined by the natural gas price, and the revenues from selling power at the market price. Thus it determines the economic value of power plants that are used to transform gas into electricity. In day-to-day operations, the plant operator generally consumes a particular gas unit only if the electricity spot price is greater than the cost of generating that unit. If the generation profit is negative, it would be unreasonable to burn a valuable commodity such as gas to obtain a low-valued product such as electricity. One would instead sell gas in the market, buy power, and stop running the plant. The flexibility of turning the plant on and

off, based on market prices, represents a real option for the asset owner and the power plant can be evaluated as a strip of European spark spread options. For an example of investment valuation using spark spread options, see [Fusai and Roncoroni \(2008\)](#) and [Luciano \(2008\)](#).

- Eventually, the spread between the hourly day-ahead electricity prices of different countries is another important spread in energy markets and a crucial quantity when evaluating an interconnection capacity contract. An interconnector is an asset that gives the owner the option to transmit electricity between two locations. In financial terms, the value of an interconnector is the same as a strip of real options written on the spread between power prices in two markets. The application of spread options in the modeling and valuation of interconnector capacity contracts is discussed in [Cartea and Pedraz \(2012\)](#).
- Selling (buying) a country's equity index in exchange for equity investments during a stock market crash (boom) is analogous to exercising an option to exchange an underperforming country (global benchmark) index for a global benchmark (country) index. This idea is exploited in [Miller \(2013\)](#) to study how effects of a crisis might be hedged.
- Another example is due to [Madan \(2009\)](#) and [Eberlein and Madan \(2012\)](#). They describe the balance sheet risks permitting random liabilities and assets on which they can perform equity value computations. This leads them to price equity as a spread option, generalizing the credit risk Merton model to stochastic debt.

The use of spread options is widespread despite the fact that pricing and hedging techniques are still underdeveloped, because, depending on the stock model we consider, the pricing problem is or is not solvable in closed form. In the Bachelier stock model, the price vector is assumed to evolve according to a bivariate Brownian motion and the option price is easily computable in closed form. If, instead, we assume prices that evolve according to a bivariate geometric Brownian motion and a zero option strike, we obtain the celebrated [Margrabe \(1978\)](#) formula. The important case in which the strike is not equal to zero does not have an explicit solution and few methods have been developed, such as the numerical integration proposed in [Ravindran \(1993\)](#) and the

popular approximation given by the formula of [Kirk \(1995\)](#), which is the current market standard. [Carmona and Durrelman \(2003a\)](#) obtain an analytical approximation formula using a family of lower bounds and propose as well an upper bound. The two bounds return a price range that is very tight for certain parameter values. [Deng et al. \(2008\)](#) approximate the spread option price and its Greeks as a sum of one-dimensional integrals following the method developed by [Pearson \(1995\)](#). [Venkatramana and Alexander \(2011\)](#) propose a closed-form approximation expressing the price of a spread option as the sum of the prices of two compound options. [Deelstra et al. \(2010\)](#) develop approximation formulas based on comonotonicity theory and moment matching methods. Finally, [Bjerksund and Stensland \(2011\)](#) propose a lower bound, showing that their formula is more accurate than Kirk's approximation. All these approximations strongly depend on the assumption that prices evolve according to a bivariate log-normal process.

Very little is discussed in the literature about the pricing of spread options in a non-Gaussian setup. Some asset classes, for example, energy price, require models with mean reversion and jumps and pricing spread options in such situations can be challenging. A Fourier transform was originally proposed by [Dempster and Hong \(2002\)](#), who implement a valuation method based on the fast Fourier transform (FFT), applying the idea of [Carr and Madan \(2000\)](#). An FFT technique is also applied by [Hurd and Zhou \(2010\)](#), who propose a pricing method based on an explicit formula for the Fourier transform of the spread option payoff in terms of the gamma function. Their formula requires a bivariate Fourier inversion. [Cheang and Chiarella \(2011\)](#) generalize Margrabe's formula to jump diffusion dynamics of the type originally introduced by [Merton \(1976\)](#) but do not discuss the non-zero strike case and do not provide numerical examples. Closed form distribution free bounds and optimal hedging strategies for spread options are derived in [Laurence and Wang \(2008\)](#). However these bounds do not appear to be very tight.

The main contribution of the present work is the derivation of a lower bound, as in [Bjerksund and Stensland \(2011\)](#), but for general processes. The only quantity we need to know explicitly is the joint characteristic function of the log-returns of the two assets. In addition, the computation

of our lower bound requires a univariate Fourier inversion, as opposed to the bivariate inversion required by [Dempster and Hong \(2002\)](#) and [Hurd and Zhou \(2010\)](#). Finally, our bound turns out to be extremely accurate and easily computable. Our lower approximation improves on the currently best available spread option pricing method we are aware of, i.e. [Hurd and Zhou \(2010\)](#), on three issues: 1. It provides an exact formula for exchange options extending to non-Gaussian models the celebrated Margrabe formula, whilst the [Hurd and Zhou \(2010\)](#) formula does not cope with the zero-strike case; 2. It can deal with mean reverting models, an important class of models that cannot be captured by the [Hurd and Zhou \(2010\)](#) formula; 3. it requires an univariate Fourier inversion, rather a bivariate one, and this implies that the computation is much faster. On the other side, whilst the [Hurd and Zhou \(2010\)](#) formula is exact, our formula provides a lower bound that is however very accurate (in general, at least four digits) across a variety of models and parametrizations.

To this regard we apply it to different non-Gaussian models, such as jump diffusion models with different jump size distributions, multivariate stochastic volatility models, mixtures of variance gamma (VG), and a VG time changed model. Mean-reverting models with jumps are also considered. Numerical examples are discussed for all these cases and benchmarked against Monte Carlo simulation. Our formula provides also a ready to use control variate estimate that allows us to achieve a very high accuracy even in the Monte Carlo simulation. As addition, our approximation becomes exact in the zero-strike case, extending to the non Gaussian case the [Margrabe \(1978\)](#) formula.

The second contribution of this work is the derivation of a tight upper bound based on the price of a new contract, the quadratic spread option. As for the lower bound, it can be computed for very general processes, provided that the bivariate characteristic function is known in closed form.

The paper outline is as follows. Section 2 generalizes the lower bound of [Bjerk Sund and Stensland \(2011\)](#) to non-Gaussian models. Section 3 compares the lower bound with the method of [Hurd and Zhou \(2010\)](#). Section 4 derives a new general upper bound. Section 5 examines in more detail the

bivariate geometric Brownian motion model, discussing two additional bounds: an improved lower bound and a second upper bound, obtained following ideas used by [Rogers and Shi \(1995\)](#) and by [Nielsen and Sandmann \(2003\)](#) for Asian options. The new lower bound represents an improvement of the Bjerksund–Stensland (BS) bound, but from a practical point of view the improvement is negligible. Section 6 briefly reviews several non-Gaussian stochastic dynamic models used in financial applications. Section 7 presents numerical experiments based on these models and show that an extended version of the BS lower bound and our new upper bound provide a very tight interval for the spread option price. Section 8 concludes the paper.

2. The lower bound

Let $S_1(t)$ and $S_2(t)$ be two stock price processes. An European spread option pays at the maturity date T the amount

$$C_K(T) = (S_1(T) - S_2(T) - K)^+.$$

The time 0 no-arbitrage fair price of the spread option is

$$C_K(0) = e^{-rT} \mathbb{E}[(S_1(T) - S_2(T) - K)^+], \quad (1)$$

where the expectation is with respect to a risk-neutral measure and r is the riskless interest rate. Here, we have used the usual notation x^+ for the positive part of x , that is, $x^+ = \max\{x, 0\}$. If $K = 0$ and $S_1(t), S_2(t)$ are jointly log-normal, computation of (1) provides the so-called [Margrabe \(1978\)](#) exchange option formula. Very little regarding non-zero strikes and non-Gaussian processes is discussed in the literature, despite the relevance of a closed pricing formula in a number of financial applications, such as those previously described.

We now present our lower bound, extending to a non Gaussian framework the idea of [Bjerksund](#)

and Stensland (2011). Let us define the event A

$$A = \left\{ \omega : \frac{S_1(T)}{S_2^\alpha(T)} > \frac{e^k}{\mathbb{E}(S_2^\alpha(T))} \right\} \quad (2)$$

and let us consider the following lower bound to the spread option payoff:

$$(S_1(T) - S_2(T) - K)^+ \geq (S_1(T) - S_2(T) - K) 1_{(A)}. \quad (3)$$

Bjerk Sund and Stensland (2011) are able to explicitly compute

$$C_K^{k,\alpha}(0) = e^{-rT} \mathbb{E}[(S_1(T) - S_2(T) - K) 1_{(A)}] \quad (4)$$

in the log-normal case. They also show that $C_K^{k,\alpha}(0)$ is a very good approximation to the exact spread option price $C_K(0)$ for suitable choices of the parameters α and k . In particular, they show that their formula in the log-normal setup is more accurate than Kirk's approximation.

We now generalize their result to a general bivariate stock price dynamic, provided that the joint characteristic function of $(\ln S_1(T), \ln S_2(T))^\top$ is available in closed form. A number of interesting models for which this is true are presented in section 6. Let $\mathbf{u} = (u_1, u_2)^\top \in \mathbb{R}^2$ and $\mathbf{X}(t) = (\ln S_1(t), \ln S_2(t))^\top$ and consider the joint characteristic function

$$\Phi_T(\mathbf{u}) = \Phi_T(u_1, u_2) = \mathbb{E} \left[e^{iu_1 \ln S_1(T) + iu_2 \ln S_2(T)} \right] = \mathbb{E} \left[e^{i\mathbf{u}^\top \mathbf{X}(T)} \right].$$

Our main result is stated in the following proposition.

Proposition 1. *The approximate spread option value $C_K^{k,\alpha}(0)$ is given in terms of a Fourier inversion formula as*

$$C_K^{k,\alpha}(0) = \left(\frac{e^{-\delta k - rT}}{\pi} \int_0^{+\infty} e^{-i\gamma k} \Psi_T(\gamma; \delta, \alpha) d\gamma \right)^+, \quad (5)$$

where

$$\begin{aligned} \Psi_T(\gamma; \delta, \alpha) = & \frac{e^{i(\gamma-i\delta) \ln(\Phi_T(0, -i\alpha))}}{i(\gamma - i\delta)} [\Phi_T((\gamma - i\delta) - i, -\alpha(\gamma - i\delta)) \\ & - \Phi_T(\gamma - i\delta, -\alpha(\gamma - i\delta) - i) \\ & - K\Phi_T(\gamma - i\delta, -\alpha(\gamma - i\delta))] \end{aligned}$$

and

$$\alpha = \frac{F_2(0, T)}{F_2(0, T) + K}, \quad (6)$$

$$k = \ln(F_2(0, T) + K). \quad (7)$$

Proof: See [Appendix A](#).

A few remarks can be made about the above formula. First, the quantity $F_2(0, T) = \mathbb{E}[S_2(T)]$ in formulas (7) and (8) is the forward price of the second asset at time 0 for delivery at future date T . Using the characteristic function properties, we can write $F_2(0, T) = \Phi_T(0, -i)$. The parameter δ tunes an exponentially decaying term introduced to allow the integration in the Fourier space, as in [Carr and Madan \(2000\)](#) and [Dempster and Hong \(2002\)](#).

Second, if the characteristic function $\Phi_T(\mathbf{u})$ is known analytically, then the Fourier transform of the lower bound can be expressed in closed form via the function $\Psi_T(\gamma; \delta, \alpha)$ in (6). The integral in (5) can be easily computed using standard numerical quadratures (NIntegrate in Mathematica or quadgk in Matlab) or via the FFT algorithm.

The main point concerning the above formula is that the approximated option price is obtained through a univariate Fourier inversion, while, for example, [Hurd and Zhou \(2010\)](#) propose an analytical formula based on the complex gamma function and requiring a bivariate Fourier inversion. Indeed, these authors consider a double Fourier transform with respect to the log-price of the two assets, while we use a Fourier transform with respect to the parameter k controlling the slope of the frontier of the exercise set A , as discussed below. Although our formula is supposed to be a lower bound to the exact price, our bound turns out to be so tight that in practice it provides an estimate that is indistinguishable from the true price. This will be discussed in more detail via an extensive

set of numerical examples on very different stochastic models, see section 7.

A fourth point relates to the choice of the free parameters, α and k . In theory, we could maximize the lower bound with respect to these parameters. Again, in practice, this is not necessary because the educated guesses proposed by [Bjerk Sund and Stensland \(2011\)](#) for the log-normal setting and generalized here to the non-Gaussian case, expressions (7) and (8), turn out to be very effective.

The fifth remark relates to the positive part in formula (5). The positive part is necessary because the original [Bjerk Sund and Stensland \(2011\)](#) formulation can give negative prices for deeply out-of-the-money options. In this case, we adopt a practical approach and set the value of the spread option to zero.

The approximation can also be applied to the Greeks. For example, assuming that interchange of differentiation and integration is allowed, the formula for the first-order sensitivity to a change in a risk factor Υ (such as underlying spot prices or model parameters) takes the form²

$$\frac{\partial C_K^{k,\alpha}(0)}{\partial \Upsilon} = \frac{e^{-\delta k - rT}}{\pi} \mathbf{1}_{\left(\int_0^{+\infty} e^{-iyk} \Psi_T(\gamma; \delta, \alpha) d\gamma \geq 0\right)} \int_0^{+\infty} e^{-iyk} \frac{\partial \Psi_T(\gamma; \delta, \alpha)}{\partial \Upsilon} d\gamma,$$

The computation of the option theta (sensitivity to the time-to-maturity) returns

$$\frac{\partial C_K^{k,\alpha}(0)}{\partial T} = \frac{e^{-\delta k - rT}}{\pi} \mathbf{1}_{\left(\int_0^{+\infty} e^{-iyk} \left(\frac{\partial \Psi_T(\gamma; \delta, \alpha)}{\partial T} - r\Psi_T(\gamma; \delta, \alpha)\right) d\gamma \geq 0\right)} \int_0^{+\infty} e^{-iyk} \left(\frac{\partial \Psi_T(\gamma; \delta, \alpha)}{\partial T} - r\Psi_T(\gamma; \delta, \alpha)\right) d\gamma.$$

For a better understanding of the approximation, we can examine Figure 1. If we define the true exercise set

$$B = \{\omega : S_1(T) \geq S_2(T) + K\},$$

²In writing the derivative, we assume that α and k in (7) and (8) are independent from the risk factor. This could be a problem in computing the option Delta with respect to the second asset and the option Theta, but numerical tests reveal that this approximation does not affect the accuracy of such Greeks, see section 7.

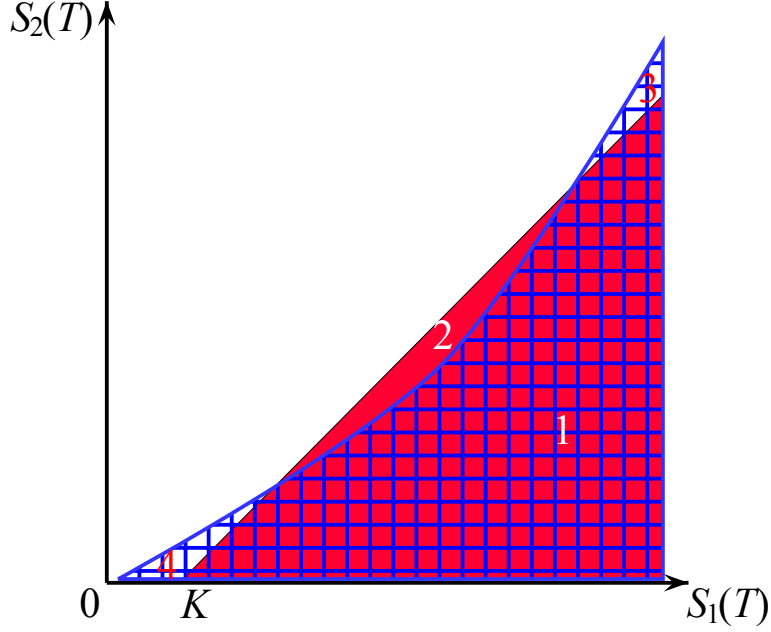


Figure 1: The true exercise region B (red) and its approximation A (blue grid).

the approximation replaces the set B by the set A defined in (2). In particular, the set A can be rewritten as

$$A = \left\{ \omega : S_1(T) \geq e^k \frac{S_2^\alpha(T)}{\mathbb{E}[S_2^\alpha(T)]} \right\}.$$

We can identify four regions in Figure 1. In region 1, sets A and B overlap and the true and approximate payoffs are equal. In region 2, the true payoff is positive but small—indeed, $S_1(T)$ is only slightly greater than $S_2(T) + K$ —while the approximated payoff is zero. In regions 3 and 4, the option payoff is zero while the approximated payoff is slightly negative. In the remaining, white region, both payoffs are zero. The role of the free parameters k is to control the slope of the frontier of the approximating exercise region A , while the parameter α controls both slope and curvature.

As final remark, we observe that if $K = 0$, it follows that $\alpha = 1$ and $k = \ln(\Phi_T(0, -i))$, so that $A \equiv B$, i.e. the two exercise regions overlap, and the approximated formula (5) gives the exact fair value of the exchange option. Therefore our approximation becomes *exact* in the zero-strike case, providing an extension of the [Margrabe \(1978\)](#) formula to a non Gaussian setting:

Proposition 2. *The exchange option with payoff $(S_1(T) - S_2(T))^+$ has price $C_0(0)$*

$$C_0(0) = C_0^{\ln(F_2(0,T)),1}(0).$$

3. A comparison with the [Hurd and Zhou \(2010\)](#) formula

[Hurd and Zhou \(2010\)](#) proposed an exact formula for spread options also based on Fourier transforms, and nowadays it appears to be the best method we are aware of. They consider the option payoff $(e^{x_1} - e^{x_2} - 1)^+$, that can be reconducted to the general case $K \neq 0$ by using scaling and interchange of $S_1(T)$ and $S_2(T)$. Their method is applicable to models in which the joint characteristic function of the two underlyings is known analytically and, for any $t > 0$, the increment $\mathbf{X}(t) - \mathbf{X}(0)$ is independent of $\mathbf{X}(0)$. This implies that the characteristic function of \mathbf{X}_T must factorize as

$$\Phi_T(\mathbf{u}) = e^{i\mathbf{u}^\top \mathbf{X}(0)} \varphi_T(\mathbf{u}), \quad \varphi_T(\mathbf{u}) := \mathbb{E} \left[e^{i\mathbf{u}^\top (\mathbf{X}(T) - \mathbf{X}(0))} \right], \quad (8)$$

where $\varphi_T(\mathbf{u})$ is independent of $\mathbf{X}(0)$. The value of the spread option can be then computed as a bivariate integration in the complex plane

$$C_K^{HZ}(0) = \frac{1}{(2\pi)^2} e^{-rT} \int \int_{\mathbb{R}^2 + i\epsilon} e^{i\mathbf{u}^\top \mathbf{X}(0)} \varphi_T(\mathbf{u}) \hat{P}(\mathbf{u}) d^2 \mathbf{u}, \quad (9)$$

where

$$\hat{P}(\mathbf{u}) = \frac{\Gamma(i(u_1 + u_2) - 1) \Gamma(-iu_2)}{\Gamma(iu_1 + 1)},$$

and Γ is the complex gamma function.

We identify the following merits of our lower bound formula $C_K^{k,\alpha}(0)$ with respect to the exact one $C_K^{HZ}(0)$:

1. The [Hurd and Zhou \(2010\)](#) formula cannot be applied when $K = 0$, while $C_K^{k,\alpha}(0)$ provides an *exact* solution to the exchange option value.
2. The assumption in formula (9) rules out mean-reverting processes that often arise in energy

applications, e.g. the model discussed in section 6.4. Our lower bound does not have such a limitation.

3. The computation of $C_K^{HZ}(0)$ requires a bivariate Fourier inversion while the approximated option price $C_K^{k,\alpha}(0)$ is obtained through a univariate Fourier inversion. Applying a Gauss–Kronrod quadrature rule to solve formula (5), the spread option value is computed much faster than using formula (10). We compare the performance of the two methods over different asset price models in section 7.

4. The upper bound

In order to control the error of the approximation in (5), we are also able to provide here an estimate of an upper bound of the spread option price. Consider the quadratic spread option payoff

$$Q(T) = \frac{1}{2} (S_1(T) - S_2(T) - L)^2 \mathbf{1}_{(S_1(T) \geq S_2(T))},$$

where $L \in \mathbb{R}$ and its choice will be discussed at the end of this section. Notice that the exercise region is the same as for an exchange option, that is, a spread option with zero strike. The price of this new contract is given in the following proposition.

Proposition 3. *The no-arbitrage price $Q(0)$ of the quadratic spread option is given by the formula*

$$Q(0) = \frac{e^{-rT}}{2} \mathbb{E} \left[(S_1(T) - S_2(T) - L)^2 \mathbf{1}_{(S_1(T) \geq S_2(T))} \right] \quad (10)$$

$$= e^{-\delta k - rT} \frac{1}{2\pi} \int_0^{+\infty} e^{-i\gamma k} \Xi_T(\gamma; \delta, \alpha) d\gamma, \quad (11)$$

where

$$\begin{aligned} \Xi_T(\gamma; \delta, \alpha) = & \frac{e^{i(\gamma - i\delta) \ln(\Phi_T(0, -i\alpha))}}{i(\gamma - i\delta)} \left[\Phi_T((\gamma - i\delta) - 2i, -\alpha(\gamma - i\delta)) \right. \\ & + \Phi_T(\gamma - i\delta, -\alpha(\gamma - i\delta) - 2i) \\ & + L^2 \Phi_T(\gamma - i\delta, -\alpha(\gamma - i\delta)) \\ & - 2L \Phi_T(\gamma - i\delta - i, -\alpha(\gamma - i\delta)) \\ & + 2L \Phi_T(\gamma - i\delta, -\alpha(\gamma - i\delta) - i) \\ & \left. - 2 \Phi_T(\gamma - i\delta - i, -\alpha(\gamma - i\delta) - i) \right] \end{aligned}$$

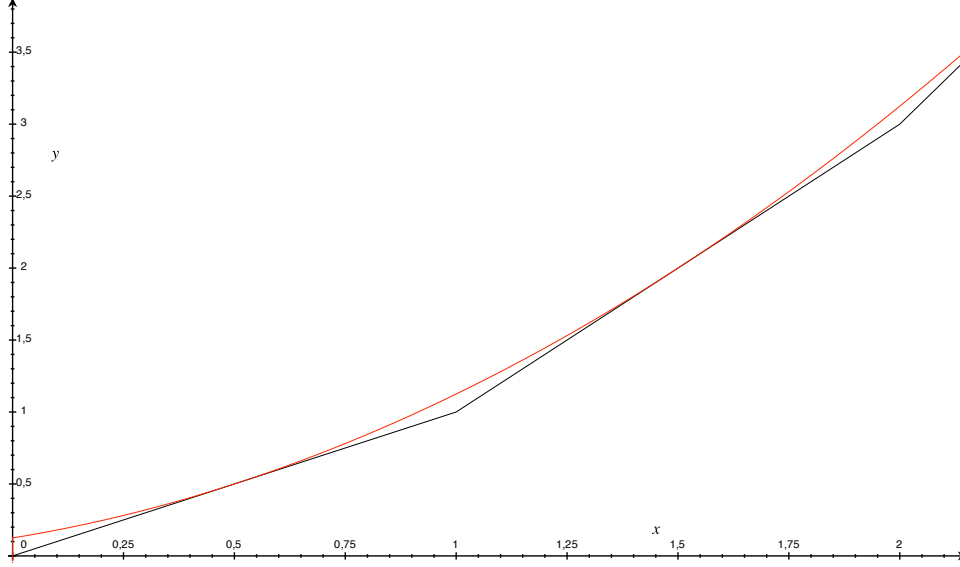


Figure 2: Comparison of the payoff $q(x)$ (red line) and the sub-replicating strategy $\pi(x)$ (black line). Here $x = S_1(T) - S_2(T)$, $\Delta K = 1$, $N = 3$ and $L = -0.5$.

and $\alpha = 1$ and $k = \ln(F_2(0, T))$.

Proof: See [Appendix B](#).

Let us consider the function

$$\pi(x) = \Delta K \sum_{j=1}^N \max(x - \Delta K(j - 0.5) - L, 0),$$

where $\Delta K > 0$, $N \in \mathbb{N}^+$ and $L \in \mathbb{R}$. We observe that the function $\pi(x)$ and the payoff $q(x) = \frac{1}{2}(x - L)^2 1_{(x \geq 0)}$ are tangent in N points, exactly in $x_j = L + j\Delta K$. In addition $q(x) \geq \pi(x)$ if $\Delta K(j - 0.5) + L \geq 0$ for $j = 1, \dots, N$. This is shown in Figure 2. If we set $x = S_1(T) - S_2(T)$, $\pi(x)$ is nothing more than a portfolio of spread options with varying strikes $K_j = \Delta K(j - 0.5) + L$ and each option is held for an amount equal to ΔK . We also require $K_j \geq 0$ for $j = 1, \dots, N$. The fair value of this portfolio is

$$\Pi(0) = e^{-rT} \mathbb{E} [\pi(S_1(T) - S_2(T))] = \Delta K \sum_{j=1}^N C_{K_j}(0)$$

and clearly $Q(0) \geq \Pi(0)$, $Q(0)$ being the fair value of the payoff $q(S_1(T) - S_2(T))$.

Suppose we are interested in pricing a spread option having strike $K_{\bar{j}} > 0$ ³, with $K_{\bar{j}} \in \{K_1, \dots, K_N\}$.

We can write

$$Q(0) \geq \Pi(0) = \Delta K \left(\sum_{j \neq \bar{j}} C_{K_j}(0) + C_{K_{\bar{j}}}(0) \right) \geq \Delta K \left(\sum_{j \neq \bar{j}} C_{K_j}^{\alpha_j, k_j}(0) + C_{K_{\bar{j}}}(0) \right),$$

where the true prices $C_{K_j}(0)$ of the spread options in the first sum are replaced by our lower bound $C_{K_j}^{\alpha_j, k_j}(0)$ in the second sum and where $\alpha_j = \frac{\Phi_T(0, -i)}{\Phi_T(0, -i) + K_j}$ and $k_j = \ln(\Phi_T(0, -i) + K_j)$. Rearranging terms, it follows that an upper bound for the spread option is given by

$$C_{K_{\bar{j}}}(0) \leq \frac{Q(0)}{\Delta K} - \sum_{j \neq \bar{j}} C_{K_j}^{\alpha_j, k_j}(0) := U_{K_{\bar{j}}}^{N, \Delta K}(0). \quad (12)$$

The computation of the upper bound $U_{K_{\bar{j}}}^{N, \Delta K}(0)$ requires the value of the deal $Q(0)$, given in formula (11), and the pricing of $N-1$ spread option contracts via the lower bound approximation in formula (5). Numerical examples show that this upper bound is extremely accurate.

The choice of the parameter L is not unique. We must guarantee that $K_{\bar{j}} \in \{K_1, \dots, K_N\}$ so every L of the form $K_{\bar{j}} - \Delta K(j - 0.5)$ is a possible candidate for $j = 1, \dots, N$. A second condition is $K_j \geq 0$ for $j = 1, \dots, N$, that is verified if and only if $K_1 = L + \Delta K/2 \geq 0$. It follows that

$$1 \leq j \leq \min \left(\left\lfloor 1 + \frac{K_{\bar{j}}}{\Delta K} \right\rfloor, N \right).$$

In our experiments we set $\bar{j} = \min \left(\left\lfloor 1 + \frac{K_{\bar{j}}}{\Delta K} \right\rfloor, N \right)$ and $L = K_{\bar{j}} - \Delta K(\bar{j} - 0.5)$.

5. The geometric Brownian motion case

This section discusses in more detail the geometric Brownian motion case and presents a derivation of the BS lower bound via the conditional expectation. More importantly, we also provide a stricter

³If the strike is strictly negative, the option is a put option written on $S_2(T) - S_1(T)$ and having strike $-K$. The put price can be then obtained by the put-call parity. If the strike is equal to zero, the lower bound provides the exact value of the exchange option.

lower bound and two analytical upper bounds. The first is computed using the power spread argument of the previous section and the second exploiting ideas used by [Rogers and Shi \(1995\)](#) and by [Nielsen and Sandmann \(2003\)](#) for Asian options.

In the bivariate Black–Scholes model (see [Black and Scholes \(1973\)](#)), the stock price vector $\mathbf{S}(t)$ has components

$$S_j(t) = S_j(t) \exp \left[\left(r - \delta_j - \sigma_j^2/2 \right) t + \sigma_j W_j(t) \right], \quad j = 1, 2 \quad (13)$$

where $\sigma_1, \sigma_2 > 0$, and W_1, W_2 are risk-neutral Brownian motions with instantaneous correlation ρ , $|\rho| < 1$, r is the risk-free rate, and δ_j is the dividend yield or the instantaneous convenience yield, depending on the nature of the underlying asset. If we consider spread options on futures, we have to set $\delta_1 = \delta_2 = r$. We denote the joint distribution of the bivariate random vector $(S_1(T), S_2(T))$ as $\mathcal{MLN}(m, V)$, where

$$m = \begin{pmatrix} \ln S_1(t) + (r - \delta_1 - \sigma_1^2/2)(T - t) \\ \ln S_2(t) + (r - \delta_2 - \sigma_2^2/2)(T - t) \end{pmatrix}, \quad V = T \begin{pmatrix} \sigma_1^2 & \rho\sigma_1\sigma_2 \\ \rho\sigma_1\sigma_2 & \sigma_2^2 \end{pmatrix},$$

With both $S_1(t)$ and $S_2(t)$ being log-normal, there is no known general formula for the spread option value except when $K = 0$, where the spread option collapses into an option to exchange one asset for another. The option value in this case is given by the formula of [Margrabe \(1978\)](#). In the general case, however, we must rely on either approximation formulas or numerical methods, such as the Gaussian quadrature as in [Ravindran \(1993\)](#). Approximation formulas allow quick calculations and facilitate analytical tractability, whereas numerical methods typically produce more accurate results. Practitioners are very focused on simple calculations and real-time solutions; hence a closed-form approximation formula is typically the preferred alternative. In this modeling framework the standard market practice is given by the approximation of [Kirk \(1995\)](#). [Bjerkstrand and Stensland \(2011\)](#) propose a new lower bound, showing their approximation is more accurate than Kirk’s formula.

Let us consider the dynamics in (14). We provide here a different derivation of the mentioned lower bound via conditional expectation. Define

$$R(t) = \frac{S_1(t)}{S_2(t)^\alpha} = \frac{S_1(0)}{S_2(0)^\alpha} e^{t(r - \delta_1 - \sigma_1^2/2 - \alpha(r - \delta_2 - \sigma_2^2/2)) + \sigma_1 W_1(t) - \alpha \sigma_2 W_2(t)},$$

and set

$$\sqrt{t} \sigma_R Z = \sigma_1 W_1(t) - \alpha \sigma_2 W_2(t), \quad \sigma_R^2 = \sigma_1^2 - 2\rho\alpha\sigma_1\sigma_2 + \alpha^2\sigma_2^2, \quad Z \sim \mathcal{N}(0, 1).$$

We can rewrite the set A as

$$\begin{aligned} A &= \left\{ \omega : R(T) > \frac{e^k}{\mathbb{E}[S_2^\alpha(T)]} \right\} \\ &= \left\{ \omega : Z \geq d = \frac{k - \ln(R(0)\mathbb{E}[S_2^\alpha(T)]) - T(r - \delta_1 - \sigma_1^2/2 - \alpha(r - \delta_2 - \sigma_2^2/2))}{\sqrt{T}\sigma_R} \right\}. \end{aligned} \quad (14)$$

If we set $U = S_1(T) - S_2(T) - K$, the BS lower bound can be equivalently rewritten as

$$\mathbb{E}[U^+] \geq \mathbb{E}[U \mathbf{1}_{(A)}]^+ = \mathbb{E}[\mathbb{E}[U|Z] \mathbf{1}_{(Z \geq d)}]^+.$$

We observe that $(W_1(T), W_2(T)|Z)^\top \sim \mathcal{MN}(\mu, \Sigma)$, where

$$\mu = \sqrt{T}Z \begin{pmatrix} a_1 \\ a_2 \end{pmatrix}, \quad \Sigma = T \begin{pmatrix} 1 - a_1^2 & \rho - a_1 a_2 \\ \rho - a_1 a_2 & 1 - a_2^2 \end{pmatrix}, \quad a_1 = \frac{\sigma_1 - \rho\alpha\sigma_2}{\sigma_R}, \quad a_2 = \frac{\sigma_1\rho - \alpha\sigma_2}{\sigma_R},$$

and therefore it follows that $(S_1(T), S_2(T)|Z)^\top \sim \mathcal{MLN}(\hat{\mu}, \hat{\Sigma})$, where

$$\hat{\mu} = \begin{pmatrix} \ln S_1(0) + (r - \delta_1 - \sigma_1^2/2)T + \sigma_1 a_1 \sqrt{T}Z \\ \ln S_2(0) + (r - \delta_2 - \sigma_2^2/2)T + \sigma_2 a_2 \sqrt{T}Z \end{pmatrix},$$

$$\hat{\Sigma} = T \begin{pmatrix} \sigma_1^2 (1 - a_1^2) & \sigma_1 \sigma_2 (\rho - a_1 a_2) \\ \sigma_1 \sigma_2 (\rho - a_1 a_2) & \sigma_2^2 (1 - a_2^2) \end{pmatrix}.$$

We can now compute the approximated payoff expectation

$$\begin{aligned} & \mathbb{E} [\mathbb{E} [U|Z] 1_{(Z \geq d)}]^+ \\ = & \mathbb{E} \left[\left(e^{\ln S_1(0) + (r - \delta_1 - \sigma_1^2 a_1^2 / 2)T + \sigma_1 a_1 \sqrt{T}Z} - e^{\ln S_2(0) + (r - \delta_2 - \sigma_2^2 a_2^2 / 2)T + \sigma_2 a_2 \sqrt{T}Z} - K \right) 1_{(Z \geq d)} \right]^+. \end{aligned}$$

By using the partial expectation property of the log-normal distribution⁴ and discounting, the above expectation gives us the BS lower bound

$$\begin{aligned} C_K^{\alpha, k}(0) &= e^{-rT} \left(S_1(0) e^{(r - \delta_1)T} N(\sigma_1 a_1 \sqrt{T} - d) \right. \\ &\quad \left. - S_2(0) e^{(r - \delta_2)T} N(\sigma_2 a_2 \sqrt{T} - d) - KN(-d) \right)^+, \end{aligned} \quad (15)$$

where $N(\cdot)$ is the cumulative density function of the standard Gaussian distribution and α and k , appearing in the definition of a_1 , a_2 , and d , can be chosen to maximize the above formula or can be set according to the guess of [Bjerk Sund and Stensland \(2011\)](#).

We now show how to improve this lower bound. We note that

$$\underbrace{\mathbb{E} [U^+]}_{\text{True price}} \geq \underbrace{\mathbb{E} [\mathbb{E} [U|Z]^+ 1_{(Z \geq d)}]}_{\text{Improved lower bound}} \geq \underbrace{\mathbb{E} [\mathbb{E} [U|Z] 1_{(Z \geq d)}]^+}_{\text{BS lower bound}}$$

so a strengthened lower bound turns out to be

$$\begin{aligned} & \mathbb{E} [\mathbb{E} [U|Z]^+ 1_{(Z \geq d)}] \\ = & \mathbb{E} \left[\left(e^{\ln S_1(0) + (r - \delta_1 - \sigma_1^2 a_1^2 / 2)T + \sigma_1 a_1 \sqrt{T}Z} - e^{\ln S_2(0) + (r - \delta_2 - \sigma_2^2 a_2^2 / 2)T + \sigma_2 a_2 \sqrt{T}Z} - K \right)^+ 1_{(Z \geq d)} \right] \\ = & \mathbb{E} \left[\left(e^{\ln S_1(0) + (r - \delta_1 - \sigma_1^2 a_1^2 / 2)T + \sigma_1 a_1 \sqrt{T}Z} - e^{\ln S_2(0) + (r - \delta_2 - \sigma_2^2 a_2^2 / 2)T + \sigma_2 a_2 \sqrt{T}Z} - K \right) 1_{(D)} \right], \end{aligned}$$

⁴This property states that for a lognormal random variable X with parameters μ and σ , we have $E(X|X > k) = e^{\mu + \frac{1}{2}\sigma^2} N\left(\frac{\mu + \sigma^2 - \ln k}{\sigma}\right)$.

where the set D is defined as

$$D \equiv \left\{ z : e^{\ln S_1(0) + (r - \delta_1 - \sigma_1^2 a_1^2 / 2)T + \sigma_1 a_1 \sqrt{T}Z} - e^{\ln S_2(0) + (r - \delta_2 - \sigma_2^2 a_2^2 / 2)T + \sigma_2 a_2 \sqrt{T}Z} - K \geq 0 \right\} \cap \{z \geq d\}.$$

The function appearing in the definition of the set D can have at most two real roots⁵ that can be numerically calculated. One of the following three situations can occur:

- (a) $D = \emptyset$;
- (b) $D = [d_1, d_2]$, where $d_1 \leq d_2$ and $d_1, d_2 \in \mathbb{R}^*$;
- (c) $D = [d_1, d_2] \cup [d_3, d_4]$, where $d_1 \leq d_2 < d_3 \leq d_4$ and $d_1, d_2, d_3, d_4 \in \mathbb{R}^*$.

Let us define a function F such that $\forall d_1 \leq d_2$ and $d_1, d_2 \in \mathbb{R}^*$, we have, $\forall x \in \mathbb{R}$,

$$F(\emptyset; x) = 0, \quad F([d_1, d_2]; x) = N(x - d_1) - N(x - d_2),$$

and, $\forall d_1 \leq d_2 < d_3 \leq d_4$ and $d_1, d_2, d_3, d_4 \in \mathbb{R}^*$, $\forall x \in \mathbb{R}$,

$$F([d_1, d_2] \cup [d_3, d_4]; x) = F([d_1, d_2]; x) + F([d_3, d_4]; x).$$

We can write the following improved lower bound in terms of F as

$$\hat{C}_K^{\alpha, k}(0) = e^{-rT} \left(S_1(0) e^{(r - \delta_1)T} F(D; \sigma_1 a_1 \sqrt{T}) - S_2(0) e^{(r - \delta_2)T} F(D; \sigma_2 a_2 \sqrt{T}) - KF(D; 0) \right).$$

Note that $C_K^{\alpha, k}(0) = \hat{C}_K^{\alpha, k}(0)$ when $D = [d_1, d_2]$ and $d_1 = d$ and $d_2 = +\infty$. From a practical perspective, this is often, but not always, the case. So in general we expect only a small improvement from adopting $\hat{C}_K^{\alpha, k}(0)$ rather than $C_K^{\alpha, k}(0)$. Numerical experiments confirm this.

Let us discuss now how to explicitly compute an upper bound that we call $U^{RS}(0)$, given that it

⁵An exponential polynomial with $N + 1$ nonzero terms, i.e. $A(z) = \sum_{j=1}^{N+1} \alpha_j e^{\lambda_j z}$ with distinct $\lambda_j \in \mathbb{R}$ and each $\alpha_j \in \mathbb{R}^*$, can have at most N real roots.

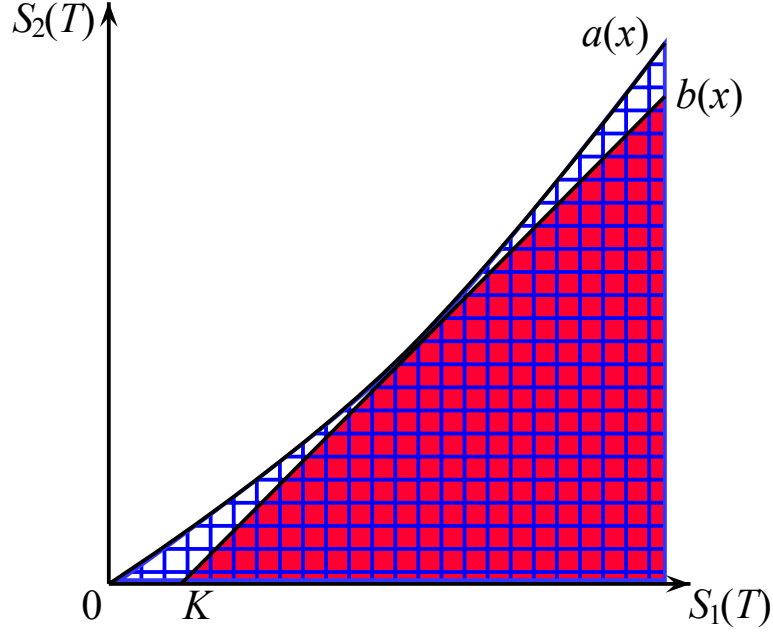


Figure 3: The true exercise region B (red) and its approximation A^{RS} (blue grid).

exploits ideas first proposed by [Rogers and Shi \(1995\)](#). Define the set

$$B = \{\omega : S_1(T) \geq S_2(T) + K\}$$

and the set A^{RS} :

$$A^{RS} = \left\{ \omega : \frac{S_1(T)}{S_2^\alpha(T)} > \frac{e^k}{\mathbb{E}[S_2^\alpha(T)]}, B \subseteq A \right\}.$$

The shape of the set A^{RS} is shown in Figure 3. Here A^{RS} is constructed requiring tangency between the function describing the exercise frontier of B , that is, $b(x) = x - K$, and the function describing the exercise frontier of A^{RS} , that is, $a(x) = \left(x \frac{\mathbb{E}[S_2(T)^\alpha]}{e^k}\right)^{1/\alpha}$. We thus have $U^+ = U^+ 1_{(A^{RS})}$ and the following equality is satisfied:

$$\mathbb{E}[U^+] - \mathbb{E}\left[\mathbb{E}\left[U 1_{(A^{RS})} | A^{RS}\right]^+\right] = \mathbb{E}\left[U^+ 1_{(A^{RS})}\right] - \mathbb{E}\left[\mathbb{E}\left[U 1_{(A^{RS})} | A^{RS}\right]^+\right].$$

Therefore, following [Nielsen and Sandmann \(2003\)](#), the error on the lower bound can be expressed

as

$$0 \leq \mathbb{E} \left[\mathbb{E} \left[U^+ \mathbf{1}_{(ARS)} | A^{RS} \right] - \mathbb{E} \left[U \mathbf{1}_{(ARS)} | A^{RS} \right]^+ \right] \leq \frac{1}{2} \mathbb{E} [\text{var}(U|Z) \mathbf{1}_{(Z>d)}]^{1/2} \mathbb{E} [\mathbf{1}_{(Z>d)}]^{1/2},$$

where d is defined in (15). The conditional variance of U is

$$\text{var}(U|Z) = \text{var}(S_1(T)|Z) + \text{var}(S_2(T)|Z) - 2\text{cov}(S_1(T), S_2(T)|Z).$$

The conditional covariance matrix between $S_1(T)$ and $S_2(T)$ is obtained exploiting properties of the log-normal distribution so that

$$\begin{aligned} \text{cov}(S_i(T), S_j(T)|Z) &= \left(e^{T\sigma_i\sigma_j(\varrho_{ij}-a_i a_j)} - 1 \right) \exp \left\{ \ln S_i(0) + \ln S_j(0) + \right. \\ &\quad \left. T \left(2r - \delta_i - \delta_j - \sigma_i^2 a_i^2 / 2 - \sigma_j^2 a_j^2 / 2 \right) + \sqrt{T} \left(\sigma_i a_i + \sigma_j a_j \right) Z \right\}, \end{aligned}$$

where ϱ_{ij} stands for the elements of the matrix

$$\varrho = \begin{pmatrix} 1 & \rho \\ \rho & 1 \end{pmatrix}.$$

The formula for the error ϵ is obtained applying again the partial expectation property of the log-normal distribution and discounting. The upper bound is therefore

$$U^{RS}(0) := \hat{C}_K^{\alpha,k}(0) + \epsilon^{\alpha,k},$$

where

$$\begin{aligned} \epsilon^{\alpha,k} &= \frac{e^{-rT}}{2} N(-d)^{1/2} \left(\sum_{i=1}^2 \sum_{j=1}^2 (-1)^{i+j} \left(e^{T\sigma_i\sigma_j(\varrho_{ij}-a_i a_j)} - 1 \right) \times \right. \\ &\quad \left. e^{\ln S_i(0) + \ln S_j(0) + T(2r - \delta_i - \delta_j + a_i a_j \sigma_i \sigma_j)} N \left(-d + \sqrt{T} \left(\sigma_i a_i + \sigma_j a_j \right) \right) \right)^{1/2}. \end{aligned}$$

This upper bound $U^{RS}(0)$ depends on the parameters α and k appearing in the definition of $d, a_1,$

and a_2 and can be minimized under the constraint $B \subseteq A^{RS}$. In practice, we have verified that, numerically, this upper bound is less tight than that obtained using the quadratic spread option argument.

In this regard, in the bivariate geometric Brownian motion case, the quantity $Q(0)$ in the upper bound $U_K^{N,\Delta K}$, given in formula (13), is equal to

$$\begin{aligned}
Q(0) = & \frac{e^{-rT}}{2} \left\{ S_1(0)^2 e^{(2r-2\delta_1+\sigma_1^2)T} N(2\sigma_1 a_1 \sqrt{T} - d) - 2LS_1(0)e^{(r-\delta_1)T} N(\sigma_1 a_1 \sqrt{T} - d) + \right. \\
& S_2(0)^2 e^{(2r-2\delta_2+\sigma_2^2)T} N(2\sigma_2 a_2 \sqrt{T} - d) + 2LS_2(0)e^{(r-\delta_2)T} N(\sigma_2 a_2 \sqrt{T} - d) - \\
& 2S_1(0)S_2(0)e^{(2r-\delta_1-\delta_2-\sigma_1 a_1/2-\sigma_2 a_2/2+\sigma_1 \sigma_2(\rho-a_1 a_2))T} N((\sigma_1 a_1 + \sigma_2 a_2) \sqrt{T} - d) + \\
& \left. L^2 N(-d) \right\}
\end{aligned}$$

In this case, we set $\alpha = 1$ and $k = \ln(\Phi_T(0, -i))$.

6. Non-Gaussian stock price models

This section presents several stock price models for which we can analyze the performance of our novel bounds. The numerical results show that bounds $C_K^{\alpha,k}(0)$ and $U_K^{N,\Delta K}(0)$ are very accurate and that, from a practical point of view, the lower bound is indistinguishable from the true price, estimated using Monte Carlo simulation. In addition our lower bound can also be used as control variate in the Monte Carlo simulation, allowing a substantial reduction in the standard error of the price estimate.

Let $\mathbf{S}(t) = (S_1(t), S_2(t))^T$ be the stock price vector and assume that the joint characteristic function of $\mathbf{X}(t) = (\ln S_1(t), \ln S_2(t))^T$ has the functional form $\Phi_T(\mathbf{u}) = e^{i\mathbf{u}^T \mathbf{X}(0)} \varphi_T(\mathbf{u})$. In the following, we set $\mathbf{e} = (1, 1)^T$. We recall at first the expression of the characteristic function in the case of geometric Brownian motion and then we present the expression of the characteristic function for a variety of non-Gaussian models.

6.1. Geometric Brownian motion

In the well-known two-asset Black–Scholes model, the vector $\mathbf{S}(t)$ has components

$$S_j(t) = S_j(0) \exp \left[\left(r - \delta_j - \sigma_j^2/2 \right) t + \sigma_j W_j(t) \right], \quad j = 1, 2,$$

where $\sigma_1, \sigma_2 > 0$, and W_1, W_2 are risk-neutral Brownian motions with instantaneous correlation $\rho, |\rho| < 1$, r is the risk-free rate, and δ_j is the continuous dividend yield paid by asset j . We have

$$\varphi_T(\mathbf{u}) = \exp \left[iT \mathbf{u}^\top \left((r - \delta) \mathbf{e} - \sigma^2/2 \right) - \mathbf{u}^\top \Sigma \mathbf{u} T/2 \right],$$

where $\Sigma = \begin{bmatrix} \sigma_1^2 & \rho \sigma_1 \sigma_2 \\ \rho \sigma_1 \sigma_2 & \sigma_2^2 \end{bmatrix}$ and $\sigma^2 = \text{diag}(\Sigma)$.

6.2. Jump diffusion model I (normally distributed jump size)

The second model we consider is the bidimensional jump diffusion model introduced by [Cheang and Chiarella \(2011\)](#). It extends the above bidimensional geometric Brownian motion by adding two jump components. The components of the stock price vector have the following functional form:

$$S_j(t) = S_j(0) \exp \left[\left(r - \delta_j - \frac{\sigma_j^2}{2} - \lambda \kappa_j - \lambda_j \kappa_{Z_j} \right) t + \sigma_j W_j(t) + \sum_{m=1}^{N_1(t)} Z_j(m) + \sum_{n=1}^{N_2(t)} Y_j(n) \right], \quad (16)$$

where $\sigma_1, \sigma_2 > 0$, and W_1, W_2 are risk-neutral Brownian motions with instantaneous correlation $\rho, |\rho| < 1$. In addition, $\sum_{m=1}^{N_1(t)} Z_1(m)$ and $\sum_{m=1}^{N_2(t)} Z_2(m)$ are univariate compound Poisson processes, driven, respectively, by the Poisson processes N_1 and N_2 with intensity rates λ_1 and λ_2 . This jump component is unique to each stock and describes the idiosyncratic shocks for that particular asset only. The idiosyncratic jump sizes Z_1 and Z_2 are independently and identically distributed according to a Gaussian distribution $\mathcal{N}(\alpha_{jj}, \xi_{jj}^2)$. The model also allows for macroeconomic shocks

in the expression

$$\sum_{n=1}^{N(t)} \mathbf{Y}(n) = \left(\sum_{n=1}^{N(t)} Y_1(n), \sum_{n=1}^{N(t)} Y_2(n) \right)^\top,$$

which is a bivariate compound Poisson process with intensity rate λ . Under the risk-neutral measure \mathbb{Q} , the jump sizes \mathbf{Y} are assumed to be independently and identically distributed according to a multivariate normal $\mathcal{MN}(\alpha, \Sigma_Y)$, where $\alpha = (\alpha_1, \alpha_2)^\top$ and

$$\Sigma_Y = \begin{pmatrix} \xi_1^2 & \rho_Y \xi_1 \xi_2 \\ \rho_Y \xi_1 \xi_2 & \xi_2^2 \end{pmatrix}.$$

Finally, the quantities κ_j and κ_{Z_j} , $j = 1, 2$ in (17) are, respectively,

$$\kappa_j = \int_{\mathbb{R}^2} [e^{y_j} - 1] m_{\mathbb{Q}}(dy) = \int_{\mathbb{R}} [e^{y_j} - 1] m_{\mathbb{Q}}(dy_j) = \exp(\alpha_j + \xi_j^2/2) - 1,$$

$$\kappa_{Z_j} = \int_{\mathbb{R}} [e^{z_j} - 1] m_{\mathbb{Q}}(dz_j) = \exp(\alpha_{jj} + \xi_{jj}^2/2) - 1.$$

The expression for the joint characteristic function is not provided in the [Cheang and Chiarella \(2011\)](#) paper. The derivation is given, by using a conditioning argument, in [Appendix C](#) and it turns out that it reads as $\Phi_T(\mathbf{u}) = e^{i\mathbf{u}^\top \mathbf{X}(0)} \varphi_T(\mathbf{u})$, where

$$\begin{aligned} \varphi_T(\mathbf{u}) = & \exp \left[T \left(i\mathbf{u}^\top \boldsymbol{\gamma} - \mathbf{u}^\top \boldsymbol{\Sigma} \mathbf{u} / 2 + \lambda_1 \left(e^{iu_1 \alpha_{11} - u_1^2 \xi_{11}^2 / 2} - 1 \right) + \lambda_2 \left(e^{iu_2 \alpha_{22} - u_2^2 \xi_{22}^2 / 2} - 1 \right) + \right. \right. \\ & \left. \left. \lambda \left(e^{i\mathbf{u}^\top \alpha - \mathbf{u}^\top \boldsymbol{\Sigma}_Y \mathbf{u} / 2} - 1 \right) \right) \right] \end{aligned} \quad (17)$$

and $\boldsymbol{\Sigma} = [\sigma_1^2, \rho\sigma_1\sigma_2; \rho\sigma_1\sigma_2, \sigma_2^2]$, $\gamma_j := r - \delta_j - \sigma_j^2/2 - \lambda\kappa_j - \lambda_j\kappa_{Z_j}$, $j = 1, 2$.

6.3. Jump diffusion model II (asymmetric Laplace distributed jump size)

The third model is the bi-dimensional jump diffusion model studied by [Huang and Kou \(2006\)](#). The difference from the previous jump diffusion model in (17) is that idiosyncratic jump sizes Z_1 and Z_2 are independently and identically distributed according to an asymmetric Laplace distribution

$\mathcal{AL}(\alpha_{jj}, \xi_{jj}^2)$ instead of being Gaussian. For a detailed description of the asymmetric Laplace distribution and its properties, see [Kotz et al. \(2001\)](#). Macroeconomic shocks N follow a compound Poisson process with intensity λ . Jump sizes \mathbf{Y} are independently and identically distributed as a multivariate asymmetric Laplace distribution $\mathcal{MAL}(\alpha, \Sigma_Y)$, where $\alpha = (\alpha_1, \alpha_2)^\top$ and

$$\Sigma_Y = \begin{pmatrix} \xi_1^2 & \rho_Y \xi_1 \xi_2 \\ \rho_Y \xi_1 \xi_2 & \xi_2^2 \end{pmatrix}.$$

In this model the quantities κ_j and κ_{Z_j} , $j = 1, 2$ are, respectively,

$$\kappa_j = \frac{1}{1 - \alpha_j - \xi_{jj}^2/2} - 1, \quad \kappa_{Z_j} = \frac{1}{1 - \alpha_{jj} - \xi_{jj}^2/2} - 1.$$

As discussed by [Huang and Kou \(2006\)](#), the joint characteristic function have the functional form $\Phi_T(\mathbf{u}) = e^{i\mathbf{u}^\top \mathbf{X}(0)} \varphi_T(\mathbf{u})$, where

$$\begin{aligned} \varphi_T(\mathbf{u}) = & \exp\left(T\left(i\mathbf{u}^\top \boldsymbol{\gamma} - \mathbf{u}^\top \Sigma \mathbf{u}/2 + \lambda_1 / \left(1 - iu_1 \alpha_{11} + u_1^2 \xi_{11}^2/2\right)\right.\right. \\ & \left. + \lambda_2 / \left(1 - iu_2 \alpha_{22} + u_2^2 \xi_{22}^2/2\right)\right) \end{aligned} \quad (18)$$

$$+ \lambda / \left(1 - i\mathbf{u}^\top \boldsymbol{\alpha} + \mathbf{u}^\top \Sigma_Y \mathbf{u}/2\right) \quad (19)$$

$$\left. - \lambda_1 - \lambda_2 - \lambda\right) \quad (20)$$

and $\Sigma = \left[\sigma_1^2, \rho\sigma_1\sigma_2; \rho\sigma_1\sigma_2, \sigma_2^2\right]$, $\boldsymbol{\gamma}_j := r - \delta_j - \sigma_j^2/2 - \lambda\kappa_j - \lambda_j\kappa_{Z_j}$, $j = 1, 2$.

6.4. Mean-reverting jump diffusion model

The fourth model is a mean-reverting jump diffusion model that generalizes the model proposed by [Hambly et al. \(2009\)](#). For $j = 1, 2$, the spot price process $S_j(t)$ is defined as the exponential of the sum of three components: a deterministic function $f_j(t)$, a Gaussian Ornstein–Uhlenbeck

process $X_j(t)$, and a mean-reverting process with a jump component $Y_j(t)$:

$$\begin{aligned} S_j(t) &= \exp\left(f_j(t) + X_j(t) + Y_j(t)\right), \\ dX_j &= -\alpha_j X_j(t)dt + \sigma_j dW_j, \\ dY_j &= -\alpha_j Y_j(t-)dt + J_j^+ dN_j^+ - J_j^- dN_j^-. \end{aligned}$$

The parameter σ_j is strictly positive and W_j is a risk-neutral Brownian motion. We assume a speed of mean reversion $\alpha_j > 0$ for both the diffusion process $X_j(t)$ and the jump process $Y_j(t)$. The two Brownian motions have instantaneous correlation ρ , $|\rho| < 1$ and N_j^+ and N_j^- are Poisson processes with intensity λ_j^+ and λ_j^- , respectively, and describe the positive and negative jump arrivals separately. The terms J_j^+ and J_j^- are independent identically distributed random variables representing the jump size and we assume they are exponentially distributed with parameters $0 < \mu_j^+ < 1$ and $\mu_j^- > 0$, respectively. Assuming independence between the jump processes, we obtain the joint characteristic function

$$\begin{aligned} \Phi_T(\mathbf{u}) &= \exp\left[iu_1 \left((X_1(0) + Y_1(0)) e^{-\alpha_1 T} + f_1(T) \right) \right. \\ &\quad + iu_2 \left((X_2(0) + Y_2(0)) e^{-\alpha_2 T} + f_2(T) \right) \\ &\quad - \frac{u_1^2 \sigma_1^2}{4\alpha_1} \left(1 - e^{-2\alpha_1 T} \right) - \frac{u_2^2 \sigma_2^2}{4\alpha_2} \left(1 - e^{-2\alpha_2 T} \right) - \rho \frac{u_1 u_2 \sigma_1 \sigma_2}{\alpha_1 + \alpha_2} \left(1 - e^{-(\alpha_1 + \alpha_2) T} \right) \\ &\quad + \frac{\lambda_1^+}{\alpha_1} \ln \left(\frac{1 - i\mu_1^+ u_1 e^{-\alpha_1 T}}{1 - i\mu_1^+ u_1} \right) + \frac{\lambda_2^+}{\alpha_2} \ln \left(\frac{1 - i\mu_2^+ u_2 e^{-\alpha_2 T}}{1 - i\mu_2^+ u_2} \right) \\ &\quad \left. + \frac{\lambda_1^-}{\alpha_1} \ln \left(\frac{1 + i\mu_1^- u_1 e^{-\alpha_1 T}}{1 + i\mu_1^- u_1} \right) + \frac{\lambda_2^-}{\alpha_2} \ln \left(\frac{1 + i\mu_2^- u_2 e^{-\alpha_2 T}}{1 + i\mu_2^- u_2} \right) \right]. \end{aligned}$$

6.5. Three-factor stochastic volatility model

The fifth model is the stochastic volatility model discussed by [Dempster and Hong \(2002\)](#) and [Hurd and Zhou \(2010\)](#). The risk-neutral dynamics of the log-price vector are given by

$$\begin{aligned} dX_1 &= (r - \delta_1 - \sigma_1^2/2)dt + \sigma_1 \sqrt{v}dW_1, \\ dX_2 &= (r - \delta_2 - \sigma_2^2/2)dt + \sigma_2 \sqrt{v}dW_2, \\ dv &= \kappa(\mu - v)dt + \sigma_v \sqrt{v}dW_v, \end{aligned}$$

where

$$\begin{aligned} \mathbb{E}[dW_1dW_2] &= \rho dt, \\ \mathbb{E}[dW_1dW_v] &= \rho_1 dt, \\ \mathbb{E}[dW_2dW_v] &= \rho_2 dt. \end{aligned}$$

The characteristic function is $\Phi_T(\mathbf{u}) = e^{i\mathbf{u}^\top \mathbf{X}(0)} \varphi_T(\mathbf{u})$, where

$$\begin{aligned} \varphi_T(\mathbf{u}) &= \exp \left[\left(\frac{2\zeta(1 - e^{-\theta T})}{2\theta - (\theta - \gamma)(1 - e^{-\theta T})} \right) v(0) + \right. \\ &\quad \left. i\mathbf{u}^\top (r\mathbf{e} - \delta)T - \frac{\kappa\mu}{\sigma_v^2} \left[2 \ln \left(\frac{2\theta - (\theta - \gamma)(1 - e^{-\theta T})}{2\theta} \right) + (\theta - \gamma)T \right] \right] \end{aligned}$$

and

$$\begin{aligned} \zeta &:= -\frac{1}{2} \left[(\sigma_1^2 u_1^2 + \sigma_2^2 u_2^2 + 2\rho\sigma_1\sigma_2 u_1 u_2) + i(\sigma_1^2 u_1 + \sigma_2^2 u_2) \right], \\ \gamma &:= \kappa - i(\rho_1\sigma_1 u_1 + \rho_2\sigma_2 u_2) \sigma_v, \\ \theta &:= \sqrt{\gamma^2 - 2\sigma_v^2 \zeta}. \end{aligned}$$

6.6. VG mixture model

The sixth model is the exponential Lévy model described by [Hurd and Zhou \(2010\)](#). A univariate VG process is a Lévy process with a Lévy characteristic triplet $(0, 0, \nu)$, where the Lévy measure is $\nu = \lambda[e^{-a_+x} \mathbf{1}_x > 0 + e^{-a_-x} \mathbf{1}_x < 0]/|x|$ for $\lambda, a_\pm > 0$. Here we consider a bivariate VG model

driven by three independent univariate VG processes Y_1, Y_2, Y with parameters $\lambda_1, \lambda_2, \lambda_Y$. Choosing $\lambda_1 = \lambda_2 = (1 - \alpha)\lambda, \lambda_Y = \alpha\lambda$, the bivariate log return process $\mathbf{X}(t) = (\ln S_1(t), \ln S_2(t))^T$ is given by the mixture

$$X_1(t) = X_1(0) + Y_1(t) + Y(t), \quad X_2(t) = X_2(0) + Y_2(t) + Y(t).$$

As discussed by [Hurd and Zhou \(2010\)](#), the joint characteristic function is given by $\Phi_T(\mathbf{u}) = e^{i\mathbf{u}^T \mathbf{X}(0)} \varphi_T(\mathbf{u})$, where

$$\begin{aligned} \varphi_T(\mathbf{u}) &= \left[1 + i \left(\frac{1}{a_-} - \frac{1}{a_+} \right) (u_1 + u_2) + \frac{(u_1 + u_2)^2}{a_- a_+} \right]^{-\alpha \lambda T} \times \\ &\quad \left[1 + i \left(\frac{1}{a_-} - \frac{1}{a_+} \right) u_1 + \frac{u_1^2}{a_- a_+} \right]^{-(1-\alpha)\lambda T} \left[1 + i \left(\frac{1}{a_-} - \frac{1}{a_+} \right) u_2 + \frac{u_2^2}{a_- a_+} \right]^{-(1-\alpha)\lambda T}. \end{aligned}$$

6.7. VG time changed model

The last model we consider is a bivariate VG process with a time change by an independent integrated CIR process. This model was introduced by [Ballotta and Bonfiglioli \(2012\)](#). The parameterization of the Lévy measure used by [Ballotta and Bonfiglioli \(2012\)](#) is

$$\nu(x) = \frac{1}{\kappa|x|} \exp \left[\frac{\theta}{\sigma^2} - |x| \frac{\sqrt{\theta^2 + 2\sigma^2/\kappa}}{\sigma^2} \right].$$

Given the parameterization above, the characteristic function of a VG process is

$$\phi(u) = -\frac{1}{\kappa} \ln \left(1 - iu\theta\kappa + u^2 \frac{\sigma^2}{2} \kappa \right). \quad (21)$$

If $Y_j(t)$, for $j = 1, 2$ are two independent VG processes with parameters $\sigma_j, \theta_j, \kappa_j$ and $Z(t)$ a third independent VG process with parameters σ_Z, θ_Z , and κ_Z , the authors introduce asset correlations considering the dynamics $G_j(t) = Y_j(t) + a_j Z(t)$, where $a_j \in \mathbb{R}$. The rate of time change of asset j

is modeled by a CIR process $v_j(s) = b_j v(t)$, where $b_j > 0$ and

$$dv(t) = k(\eta - v(t))dt + \lambda \sqrt{v(t)}dW(t)$$

and $W(t)$ is a Brownian motion common to the whole vector of time changes but independent of the base process $\mathbf{G}(t) = (G_1(t), G_2(t))^T$. The clock of asset j is assumed to be the integrated variance process $V_j(t) = b_j V(t)$, that is,

$$V_j(t) = \int_0^t v_j(s)ds.$$

Considering $B_j(t) = G_j(V_j(t))$, we define the stock price risk-neutral dynamics as

$$S_j(t) = S_j(0)e^{(r-\delta_j)t} \frac{e^{B_j(t)}}{\mathbb{E}[e^{B_j(t)}]}.$$

Assuming that $b_1 < b_2$, the joint characteristic function is given by $\Phi_T(\mathbf{u}) = e^{i\mathbf{u}^T \mathbf{X}(0)} \varphi_T(\mathbf{u})$, where

$$\varphi_T(\mathbf{u}) = \phi_T^V(-ig(u_1, u_2; a_1, a_2, b_1, b_2))e^{i\mathbf{u}^T((r\mathbf{e}-\delta)T-\mathbf{p}_T)},$$

with

$$g(u_1, u_2; a_1, a_2, b_1, b_2) = b_1 \phi^{Y_1}(u_1) + b_2 \phi^{Y_2}(u_2) + b_1 \phi^Z(u_1 a_1 + u_2 a_2) + (b_2 - b_1) \phi^Z(u_2 a_2),$$

$$\mathbf{p}_T = (\phi_T^V(-ig(-i, 0; a_1, a_2, b_1, b_2)), \phi_T^V(-ig(0, -i; a_1, a_2, b_1, b_2)))^T.$$

In the above expression the characteristic functions of Y_1, Y_2 , and Z are, respectively, indicated by ϕ^{Y_1} , ϕ^{Y_2} , and ϕ^Z and are given in equation (20), while ϕ_T^V is the characteristic function of the

integrated CIR process V that we recall here for completeness:

$$\begin{aligned}\phi_t^V(u) &= e^{A(u,t)+B(u,t)v(0)} \\ A(u,t) &= \frac{2k\eta}{\lambda^2} \ln \left(\frac{2\zeta(u)e^{\frac{\zeta(u)+k}{2}t}}{(\zeta(u)+k)(e^{\zeta(u)t}-1)+2\zeta(u)} \right) \\ B(u,t) &= \frac{2iu(e^{\zeta(u)t}-1)}{(\zeta(u)+k)(e^{\zeta(u)t}-1)+2\zeta(u)} \\ \zeta(u) &= \sqrt{k^2-2\lambda^2iu}.\end{aligned}$$

7. Numerical results

This section discusses numerical results with reference to the just presented models. Numerical experiments were coded and implemented in Matlab version 7.9.0 on an Intel Core i5 2.40 GHz machine running under Mac OS X with 4 GB physical memory. We compute the fair value of spread option contracts, spanning different strike prices, for each model presented in section 6. Numerical results are reported in Tables 1 to 7. Prices obtained via Monte Carlo simulation are used as a benchmark. To reduce the simulation error, we use the lower bound as a control variate. We rewrite equation (1) as

$$C_K(0) = C_K^{k,\alpha}(0) + e^{-rT} \mathbb{E}[(S_1(T) - S_2(T) - K)^+] - e^{-rT} \mathbb{E}[(S_1(T) - S_2(T) - K)1_{(A)}]^+.$$

We calculate $C_K^{k,\alpha}(0)$ with formula (5) and use Monte Carlo simulation to compute the two expected values, which are highly correlated. The simulation error can be reduced substantially.

The number of simulations is chosen depending on the model, as indicated in each Table. The columns labeled *C.I. length* give the length of the 95% mean-centered Monte Carlo confidence interval. In all cases the confidence interval of the control variate estimate is so small that it allows us to appreciate the accuracy of our lower bound. The lower bound is computed using the formula (5) and is displayed in the column labeled $C_K^{\alpha,k}(0)$. The integral is computed by a Gauss–Kronrod quadrature rule using Matlab’s built-in function `quadgk`. Values obtained maximizing the lower

bound with respect to α and k are presented in the column labeled $C_K^{\alpha^*, k^*}(0)$. However, we can see that the optimized lower bound does not significantly improve the approximation provided by formula $C_K^{\alpha, k}(0)$. Therefore we strongly suggest to use formula (5) with default values for α and k as in (7) and (8). **We also provide the numbers $C_K^{HZ}(0)$ computed with the method of Hurd and Zhou (2010), where parameters N^{HZ} , \bar{u} and ϵ are set as indicated in each Table, to guarantee the same accuracy as the Monte Carlo benchmark. Notice that $C_K^{HZ}(0)$ cannot be computed (N.A.) when $K = 0$ or when we consider the mean-reverting jump diffusion model (Table 4). In principle, we could price the exchange option using the Hurd and Zhou (2010) formula setting the strike equal to a very small number, but unfortunately this approximation produces very inaccurate results due to numerical instabilities, depending on the characteristic function specification. For example, given results in Table 1 and Table 7, in the geometric Brownian motion we can estimate the price of the exchange option setting $K = 10^{-6}$ in the Hurd and Zhou (2010) method. However, for the VG time changed model, the method becomes unstable for small strikes. If we limit ourselves to the choice $K = 10^{-2}$ then $C_K^{HZ}(0) = 6.285187$, when the exact price obtained via our approach turns out to be $C_K^{\alpha, k}(0) = 6.292223$.**

The upper bound is given in the column labeled $U_K^{N, \Delta K}(0)$ and is computed by setting N and ΔK as indicated in each table. Our numerical experiments show that the upper bound is quite good in all cases, albeit it does not achieve the same tightness as the lower bound, even when minimized with respect to N and ΔK . The strike price of the quadratic spread option involved in the computation of $U_K^{N, \Delta K}(0)$ is displayed in the column labeled L . The solution $C_K^{\alpha, k}(0)$ is exact in the zero-strike case, so $U_K^{N, \Delta K}(0)$ and L are not given in this case.

For the geometric Brownian motion case, in Table 1, we also present Kirk's approximation formula, the improved lower bound $\hat{C}_K^{\alpha^*, k^*}(0)$, and the Rogers–Shi-type upper bound $U^{RS}(0)$. As noted in the previous section, the lower bound $\hat{C}_K^{\alpha^*, k^*}(0)$ does not significantly improve with respect to the approximation $C_K^{k, \alpha}(0)$. In addition, the upper bound $U^{RS}(0)$, although developed ad hoc for

the geometric Brownian motion case, seems to work worse than the more general upper bound $U_K^{N,\Delta K}(0)$.

Table 8 compares the Gauss–Kronrod quadrature rule in $C_K^{\alpha,k}(0)$ and the bivariate Fourier inversion in $C_K^{HZ}(0)$ in terms of computational cost across a variety of models, using the same parameters setting as in Tables 1 to 7. Here the option strike price is set at $K = 2$. The Table gives the computational times for computing the spread option price using the two formulae and we observe that the computation of $C_K^{\alpha,k}(0)$ is considerably faster than $C_K^{HZ}(0)$ for every model by a factor varying between 130 (model 3FSV) and 190 (model JD1). However, for the love of true, we have to remark that the bivariate FFT implementation of the [Hurd and Zhou \(2010\)](#) formula provides a matrix of spread option prices. Using such a matrix, interpolation can be used to price a spread option price for $K^* \neq K$, with a additional small computational cost. Therefore, it makes a little difference in terms of computing times if we evaluate a single option or a large panel of contracts with the method of [Hurd and Zhou \(2010\)](#). On the other hand the computational cost of our lower bound increases linearly in the number of evaluated spread options, so the advantage in using formula (5) decreases as the number of contracts to be priced increases.

Table 9 compares the first order Greeks computed as discussed in Section 2 with the ones in [Hurd and Zhou \(2010\)](#). The two estimates are comparable, so our lower bound also provides accurate Greeks.

Finally, Table 10 compares the control variate (MC) and the crude (MC^{cr}) Monte Carlo for each model. The model parameters are set as in Tables 1 to 7 and the option strike price is $K = 2$ for every model. The confidence interval length of each Monte Carlo simulation is also provided. Using our lower bound as a control variate in the simulation, the standard error and therefore the confidence interval of the crude Monte Carlo estimate are significantly reduced. For example the length of the confidence interval in the geometric Brownian motion model is reduced from 1.4×10^{-2} to 3.1×10^{-7} . A substantial reduction is also obtained in the other models. For example in the time changed VG model the confidence interval length is reduced from 2.2×10^{-2} to $1.7 \times$

10^{-5} .

8. Conclusions

This paper extends the lower bound approximation for the spread option price in [Bjerk Sund and Stensland \(2011\)](#) from the geometric Brownian motion case to more general processes, allowing for jumps, stochastic volatility and mean reversion. The only quantity we need to know explicitly is the joint characteristic function of the log-returns of the two assets. The computation of our lower bound requires a univariate Fourier inversion, as opposed to the bivariate inversion required by [Hurd and Zhou \(2010\)](#) and [Dempster and Hong \(2002\)](#). Our bound is extremely accurate and easily computable. In addition it can be used as control variate in Monte Carlo simulations. This allows us to obtain very tight confidence intervals as well. An exact formula for the zero strike case as well as a tight upper bound on the estimation error are also obtained. The upper bound is based on the price of a new contract, the quadratic spread option. Many important processes in finance have a well known explicit characteristic function and can be included in the pricing method with little difficulty. A topic for further research is the extension to spread options with an early exercise feature.

Appendix A. Proof of Proposition 1

We observe that $\mathbb{E}[S_2^\alpha(T)] = \Phi_T(0, -i\alpha)$, so we can rewrite the set A defined in (2) as

$$\begin{aligned} A &= \{\omega : \ln S_1(T) - \alpha \ln S_2(T) > k - \ln \Phi_T(0, -i\alpha)\} \\ &= \{\omega : X_1(T) - \alpha X_2(T) + \ln \Phi_T(0, -i\alpha) > k\}. \end{aligned}$$

Following [Carr and Madan \(2000\)](#) and [Dempster and Hong \(2002\)](#), we multiply the expected value of the option approximation (4) by an exponentially decaying term, tuned by a parameter δ , so that it is square integrable in k over the negative axis. Then we apply the Fourier transform to this

modified lower bound price:

$$\begin{aligned}
\Psi_T(\gamma; \delta, \alpha) &= \int_{\mathbb{R}} e^{i\gamma k + \delta k} \mathbb{E}[(S_1(T) - S_2(T) - K) 1_{(A)}] dk \\
&= \int_{\mathbb{R}} e^{i\gamma k + \delta k} \left[\int_{\mathbb{R}} \int_{k - \ln \Phi_T(0, -i\alpha) + \alpha X_2(T)}^{+\infty} (e^{X_1(T)} - e^{X_2(T)} - K) f(X_1, X_2) dX_1 dX_2 \right] dk \\
&= \int_{\mathbb{R}} \int_{\mathbb{R}} \left[\int_{-\infty}^{X_1(T) + \ln \Phi_T(0, -i\alpha) - \alpha X_2(T)} e^{i\gamma k + \delta k} dk \right] (e^{X_1(T)} - e^{X_2(T)} - K) f(X_1, X_2) dX_1 dX_2 \\
&= \frac{1}{i\gamma + \delta} \int_{\mathbb{R}} \int_{\mathbb{R}} e^{i(\gamma - i\delta)(X_1(T) - \alpha X_2(T) + \ln \Phi_T(0, -i\alpha))} (e^{X_1(T)} - e^{X_2(T)} - K) f(X_1, X_2) dX_1 dX_2 \\
&= \frac{e^{i(\gamma - i\delta) \ln(\Phi_T(0, -i\alpha))}}{i(\gamma - i\delta)} \left[\mathbb{E} \left[e^{i(\gamma - i\delta - i)X_1(T) - i\alpha(\gamma - i\delta)X_2(T)} \right] - \mathbb{E} \left[e^{i(\gamma - i\delta)X_1(T) + i(-\alpha\gamma + i\alpha\delta - i)X_2(T)} \right] \right. \\
&\quad \left. - K \mathbb{E} \left[e^{i(\gamma - i\delta)(X_1(T) - \alpha X_2(T))} \right] \right] \\
&= \frac{e^{i(\gamma - i\delta) \ln(\Phi_T(0, -i\alpha))}}{i(\gamma - i\delta)} \left[\Phi_T(\gamma - i(\delta + 1), -\alpha(\gamma - i\delta)) - \Phi_T(\gamma - i\delta, -\alpha\gamma + i\alpha\delta - i) \right. \\
&\quad \left. - K \Phi_T(\gamma - i\delta, -(\gamma - i\delta)\alpha) \right].
\end{aligned}$$

The lower bound is given by an inverse transform and depends on the parameters α and k . The optimal lower bound is achieved using the maximization

$$\max_{k, \alpha} e^{-\delta k - rT} \frac{1}{\pi} \int_0^{+\infty} e^{-i\gamma k} \Psi_T(\gamma; \delta, \alpha) d\gamma.$$

In practice, the optimization can be replaced by an educated guess, as suggested by [Bjerk Sund and Stensland \(2011\)](#), setting

$$\alpha = \frac{F_2(0, T)}{F_2(0, T) + K}, \quad k = \ln(F_2(0, T) + K),$$

where $F_2(0, T)$ is the forward price of the second asset at time 0 for delivery at a future date T .

Appendix B. Proof of Proposition 3

Using the same arguments as in [Appendix A](#), we have

$$\begin{aligned}
\Xi_T(\gamma; \delta, \alpha) &= \int_{\mathbb{R}} e^{i\gamma k + \delta k} \mathbb{E} \left[(S_1(T) - S_2(T) - L)^2 1_{(A)} \right] dk \\
&= \int_{\mathbb{R}} e^{i\gamma k + \delta k} \left[\int_{\mathbb{R}} \int_{k - \ln \Phi_T(0, -i\alpha) + \alpha X_2(T)}^{+\infty} \left(e^{X_1(T)} - e^{X_2(T)} - L \right)^2 f(X_1, X_2) dX_1 dX_2 \right] dk \\
&= \int_{\mathbb{R}} \int_{\mathbb{R}} \left[\int_{-\infty}^{X_1(T) + \ln \Phi_T(0, -i\alpha) - \alpha X_2(T)} e^{i\gamma k + \delta k} dk \right] \left(e^{2X_1(T)} + e^{2X_2(T)} + L^2 - 2Le^{X_1(T)} \right. \\
&\quad \left. - 2e^{X_1(T) + X_2(T)} + 2Le^{X_2(T)} \right) f(X_1, X_2) dX_1 dX_2 \\
&= \frac{1}{i\gamma + \delta} \int_{\mathbb{R}} \int_{\mathbb{R}} e^{i(\gamma - i\delta)(X_1(T) - \alpha X_2(T) + \ln \Phi_T(0, -i\alpha))} \left(e^{2X_1(T)} + e^{2X_2(T)} + L^2 - 2Le^{X_1(T)} \right. \\
&\quad \left. - 2e^{X_1(T) + X_2(T)} + 2Le^{X_2(T)} \right) f(X_1, X_2) dX_1 dX_2 \\
&= \frac{e^{i(\gamma - i\delta) \ln(\Phi_T(0, -i\alpha))}}{i(\gamma - i\delta)} \left[\mathbb{E} \left[e^{i(\gamma - i\delta - 2i)X_1(T) - i\alpha(\gamma - i\delta)X_2(T)} \right] - \mathbb{E} \left[e^{i(\gamma - i\delta)X_1(T) + i(-\alpha\gamma + i\alpha\delta - 2i)X_2(T)} \right] \right. \\
&\quad \left. + L^2 \mathbb{E} \left[e^{i(\gamma - i\delta)(X_1(T) - \alpha X_2(T))} \right] - 2L \mathbb{E} \left[e^{i(\gamma - i\delta - i)X_1(T) - i\alpha(\gamma - i\delta)X_2(T)} \right] + \right. \\
&\quad \left. 2L \mathbb{E} \left[e^{i(\gamma - i\delta)X_1(T) + i(-\alpha\gamma + i\alpha\delta - i)X_2(T)} \right] - 2 \mathbb{E} \left[e^{i(\gamma - i\delta - i)X_1(T) + i(-\alpha\gamma + i\alpha\delta - i)X_2(T)} \right] \right] \\
&= \frac{e^{i(\gamma - i\delta) \ln(\Phi_T(0, -i\alpha))}}{i(\gamma - i\delta)} \left[\Phi_T((\gamma - i\delta) - 2i, -\alpha(\gamma - i\delta)) \right. \\
&\quad \left. + \Phi_T(\gamma - i\delta, -\alpha(\gamma - i\delta) - 2i) + L^2 \Phi_T(\gamma - i\delta, -\alpha(\gamma - i\delta)) \right. \\
&\quad \left. - 2L \Phi_T(\gamma - i\delta - i, -\alpha(\gamma - i\delta)) + 2L \Phi_T(\gamma - i\delta, -\alpha(\gamma - i\delta) - i) \right. \\
&\quad \left. - 2 \Phi_T(\gamma - i\delta - i, -\alpha(\gamma - i\delta) - i) \right].
\end{aligned}$$

We can obtain $Q(0)$ by an inverse Fourier transform, discounting and setting parameters $\alpha = 1$ and $k = \ln(F_2(0, T))$.

Appendix C. Derivation of formula (18)

The characteristic function is

$$\begin{aligned}\mathbb{E}\left[e^{i\mathbf{u}^\top \mathbf{X}(T)}\right] &= e^{i\mathbf{u}^\top (\mathbf{X}(0) + \gamma T)} \mathbb{E}\left[\exp\left\{iu_1\left(\sigma_1 W_1(T) + \sum_{m=1}^{N_1(T)} Z_1(m) + \sum_{n=1}^{N(T)} Y_1(n)\right)\right.\right. \\ &\quad \left.\left.+iu_2\left(\sigma_2 W_2(T) + \sum_{m=1}^{N_2(T)} Z_2(m) + \sum_{n=1}^{N(T)} Y_2(n)\right)\right\}\right] \\ &= e^{i\mathbf{u}^\top (\mathbf{X}(0) + \gamma T)} \sum_{n=0}^{\infty} \sum_{n_1=0}^{\infty} \sum_{n_2=0}^{\infty} \frac{e^{-\lambda T} (\lambda T)^n}{n!} \frac{e^{-\lambda_1 T} (\lambda_1 T)^{n_1}}{n_1!} \frac{e^{-\lambda_2 T} (\lambda_2 T)^{n_2}}{n_2!} \beta(n, n_1, n_2),\end{aligned}$$

where

$$\begin{aligned}\beta(n, n_1, n_2) &= \mathbb{E}\left[\exp\left\{iu_1\left(\sigma_1 W_1(T) + \sum_{m=1}^{N_1(T)} Z_1(m) + \sum_{n=1}^{N(T)} Y_1(n)\right)\right.\right. \\ &\quad \left.\left.+iu_2\left(\sigma_2 W_2(T) + \sum_{m=1}^{N_2(T)} Z_2(m) + \sum_{n=1}^{N(T)} Y_2(n)\right)\right\}\middle|N(T) = n, N_1(T) = n_1, N_2(T) = n_2\right].\end{aligned}$$

Conditioning to the event $\{N(T) = n, N_1(T) = n_1, N_2(T) = n_2\}$, $\beta(n, n_1, n_2)$ is the characteristic function of a bivariate normal variable $B(n, n_1, n_2)$, where

$$B(n, n_1, n_2) \sim \mathcal{MN}\left(\begin{pmatrix} n_1 \alpha_{11} + n \alpha_1 \\ n_2 \alpha_{22} + n \alpha_2 \end{pmatrix}, \begin{pmatrix} n_1 \xi_{11}^2 + n \xi_1^2 + \sigma_1^2 T & n \rho_Y \xi_1 \xi_2 + \sigma_1 \sigma_2 \rho T \\ n \rho_Y \xi_1 \xi_2 + \sigma_1 \sigma_2 \rho T & n_2 \xi_{22}^2 + n \xi_2^2 + \sigma_2^2 T \end{pmatrix}\right).$$

We therefore obtain

$$\begin{aligned}\beta(n, n_1, n_2) &= \exp\{iu_1(n_1 \alpha_{11} + n \alpha_1) + iu_2(n_2 \alpha_{22} + n \alpha_2) - u_1^2(n_1 \xi_{11}^2 + n \xi_1^2 + \sigma_1^2 T)/2 - \\ &\quad u_2^2(n_2 \xi_{22}^2 + n \xi_2^2 + \sigma_2^2 T)/2 - u_1 u_2(n \rho_Y \xi_1 \xi_2 + \sigma_1 \sigma_2 \rho T)\},\end{aligned}$$

which results in

$$\mathbb{E}[e^{iu^T X(T)}] = e^{iu^T(X(0)+\gamma T)-T(\lambda+\lambda_1+\lambda_2+u_1^2\sigma_1^2/2+u_2^2\sigma_2^2/2+u_1u_2\sigma_1\sigma_2)} \sum_{n_1=0}^{\infty} \frac{e^{n_1(\ln(\lambda_1 T)+iu_1\alpha_{11}-u_1^2\xi_{11}^2/2)}}{n_1!} \sum_{n_2=0}^{\infty} \frac{e^{n_2(\ln(\lambda_2 T)+iu_2\alpha_{22}-u_2^2\xi_{22}^2/2)}}{n_2!} \sum_{n=0}^{\infty} \frac{e^{n(\ln(\lambda T)+iu_1\alpha_1+iu_2\alpha_2-u_1^2\xi_1^2/2-u_2^2\xi_2^2/2-u_1u_2\xi_1\xi_2\rho\gamma)}}{n!}.$$

Straightforward calculations lead to the formula (18).

References

References

Ballotta, L., Bonfiglioli, E., 2012. Multivariate asset models using Lévy processes and applications. URL: <http://ssrn.com/abstract=1695527>. Working paper.

Bjerk Sund, P., Stensland, G., 2011. Closed form spread option valuation. *Quantitative Finance* iFirst, 1–10.

Black, F., Scholes, M., 1973. The Pricing of Option and Corporate Liabilities. *Journal of Political Economy* 81, 637–654.

Carmona, R., Durrelman, V., 2003a. Pricing and hedging spread option in a log-normal model. URL: <http://orfe.princeton.edu/~rcarmona/download/fe/spread.pdf>. Working paper.

Carmona, R., Durrelman, V., 2003b. Pricing and hedging spread options. *SIAM Review* 45.

Carr, P., Madan, D., 2000. Option valuation using the fast Fourier transform. *Journal of Computational Finance* 2, 61–73.

Cartea, A., Pedraz, C.G., 2012. How much should we pay for interconnecting electricity markets? A real options approach. *Energy Economics* 34, 14–30.

- Cheang, G.H.L., Chiarella, C., 2011. Exchange option under jump-diffusion dynamics. *Applied Mathematical Finance* 18, 245–276.
- Deelstra, G., Petkovic, A., M.Vanmaele, 2010. Pricing and hedging Asian basket spread options. *Journal of Computational and Applied Mathematics* 234, 2814–2830.
- Dempster, M.A.H., Hong, S.S.G., 2002. Spread option valuation and the fast Fourier transform, in: *Mathematical Finance—Bachelier Congress 2000*. Springer, Berlin, pp. 203–220.
- Dempster, M.A.H., Medova, E., Tang, K., 2008. Long term spread option valuation and hedging. *Journal of Banking & Finance* 32, 2530–2540.
- Deng, S., Li, M., Zhou, E., 2008. Closed-form approximation for spread option prices and Greeks. *Journal of Derivatives* 15, 58–80.
- Duan, J.C., Pliska, S.R., 2004. Option valuation with co-integrated asset prices. *Journal of Economic Dynamics & Control* 28, 727–754.
- Eberlein, E.D., Madan, D., 2012. Unbounded liabilities, capital reserve requirements and the taxpayer put option. *Quantitative Finance* 12, 709–724.
- Fusai, G., Roncoroni, A., 2008. *Implementing Models in Quantitative Finance: Methods and Cases*. Springer, Berlin.
- Girma, P.B., Paulson, A.S., 1998. Seasonality in petroleum futures spreads. *Journal of Futures Markets* 18, 581–598.
- Girma, P.B., Paulson, A.S., 1999. Risk arbitrage opportunities in petroleum futures spreads. *Journal of Futures Markets* 19, 931–955.
- Hambly, B., Howison, S., Kluge, T., 2009. Modelling spikes and pricing swing options in electricity markets. *Quantitative Finance* 9, 937–949.

- Huang, Z., Kou, S., 2006. First passage times and analytical solutions for options on two assets with jump risk. Working paper.
- Hurd, T.R., Zhou, Z., 2010. A Fourier transform method for spread option pricing. *SIAM Journal of Financial Mathematics* 1, 142–157.
- Kirk, E., 1995. Correlation in the energy market, in: *Managing energy price risk*. First ed.. Risk Publication, London, pp. 71–78.
- Kotz, S., Kozubowski, T.J., Podgorsky, K., 2001. *The Laplace Distribution and Generalizations: A Revisit With Applications to Communications, Economics, Engineering, and Finance*. Birkhauser, Boston.
- Laurence, P., Wang, T., 2008. Distribution-free upper bounds for spread options and market-implied antimonotonicity gap. *The European Journal of Finance* 14, 717–734.
- Luciano, E., 2008. Spark spread options when commodity prices are represented as time-changed processes, in: *Risk Management in Commodity Markets: From Shipping to Agriculturals and Energy*. Wiley, pp. 129–151.
- Madan, D., 2009. Capital requirements, acceptable risks and profits. *Quantitative Finance* 7, 767–773.
- Margrabe, W., 1978. The value of an option to exchange one asset for another. *Journal of Finance* 33, 177–186.
- Merton, R.C., 1976. Option pricing when underlying stock returns are discontinuous. *Journal of Financial Economics* 3, 125–144.
- Miller, S.M., 2013. Booms and busts as exchange options. *Multinational Finance Journal*, Forthcoming.
- Nielsen, J.A., Sandmann, K., 2003. Pricing bounds on Asian options. *Journal of Financial and Quantitative Analysis* 38, 449–473.

Pearson, N.D., 1995. An efficient approach for pricing spread options. *Journal of Derivatives* 3, 76–91.

Ravindran, K., 1993. Low-fat Spreads. *Risk* 6, 56–57.

Rogers, L.C.G., Shi, Z., 1995. The value of an Asian option. *Journal of Applied Probability* 32, 1077–1088.

Venkatramana, A., Alexander, C., 2011. Closed form approximations for spread options. *Applied Mathematical Finance* 18, 447–472.

| K | $C_K^{\alpha,k}(0)$ | $C_K^{\alpha^*,k^*}(0)$ | $\hat{C}_K^{\alpha^*,k^*}(0)$ | $C_K^{Kirk}(0)$ | $C_K^{HZ}(0)$ | MC | C.I. length | $U_K^{N,\Delta K}(0)$ | L | $U^{RS}(0)$ |
|-----|---------------------|-------------------------|-------------------------------|-----------------|---------------|----------|------------------------|-----------------------|-------|-------------|
| 0.0 | 8.513225 | 8.513225 | 8.5132251 | 8.513225 | N.A. | 8.513225 | 2.004×10^{-9} | N.A. | N.A. | N.A. |
| 0.4 | 8.312461 | 8.312461 | 8.312461 | 8.312461 | 8.312461 | 8.312461 | 4.466×10^{-8} | 8.330482 | 0.15 | 8.867626 |
| 0.8 | 8.114993 | 8.114993 | 8.114993 | 8.114993 | 8.114994 | 8.114994 | 9.217×10^{-8} | 8.133036 | 0.05 | 8.633288 |
| 1.2 | 7.920819 | 7.920819 | 7.920819 | 7.920819 | 7.920820 | 7.920820 | 1.640×10^{-7} | 7.938902 | -0.05 | 8.410323 |
| 1.6 | 7.729931 | 7.729931 | 7.729931 | 7.729931 | 7.729932 | 7.729933 | 2.140×10^{-7} | 7.748035 | -0.15 | 8.195125 |
| 2.0 | 7.542322 | 7.542322 | 7.542322 | 7.542322 | 7.542324 | 7.542324 | 3.088×10^{-7} | 7.560385 | -0.25 | 7.986151 |
| 2.4 | 7.357982 | 7.357982 | 7.357982 | 7.357982 | 7.357984 | 7.357984 | 3.907×10^{-7} | 7.376003 | 0.15 | 7.782577 |
| 2.8 | 7.176899 | 7.176899 | 7.176899 | 7.176899 | 7.176902 | 7.176903 | 4.861×10^{-7} | 7.194941 | 0.05 | 7.583903 |
| 3.2 | 6.999060 | 6.999060 | 6.999060 | 6.999060 | 6.999065 | 6.999065 | 5.632×10^{-7} | 7.017144 | -0.05 | 7.389794 |
| 3.6 | 6.824452 | 6.824452 | 6.824452 | 6.824452 | 6.824458 | 6.824458 | 7.138×10^{-7} | 6.842556 | -0.15 | 7.200013 |
| 4.0 | 6.653058 | 6.653058 | 6.653058 | 6.653058 | 6.653065 | 6.653065 | 7.838×10^{-7} | 6.671121 | -0.25 | 7.014377 |

Table 1: Prices of the spread option computed for strike K in the geometric Brownian motion model of section 5. The parameter values are $S_1(0) = 100$, $S_2(0) = 96$, $\rho = 0.5$, $\sigma_1 = 0.2$, $\sigma_2 = 0.1$, $\delta_1 = 0.05$, $\delta_2 = 0.05$, $r = 0.1$, $T = 1.0$, $M = 10^6$, $N = 1000$, and $\Delta K = 0.5$. Hurd and Zhou parameters are $N^{HZ} = 512$, $\bar{u} = 40$ and $\epsilon = [-3, 1]^T$. Column $C_K^{\alpha,k}(0)$ contains the lower bound in formula (5). Values in $C_K^{\alpha^*,k^*}$ are obtained maximizing the lower bound with respect to α and k . The improved lower bound of the Rogers–Shi-type is in column $\hat{C}_K^{\alpha^*,k^*}(0)$ while column $C_K^{Kirk}(0)$ presents values obtained by Kirk’s approximation formula. Results of Hurd and Zhou (2010) are shown in column $C_K^{HZ}(0)$. Columns MC and C.I. length contains respectively the Monte Carlo prices and confidence intervals. The upper bound computed using the power spread option argument is displayed in column $U_K^{N,\Delta K}$ while L shows the chosen strike of the power spread option. Finally the Rogers–Shi-type upper bound is given in column $U^{RS}(0)$.

| K | $C_K^{\alpha,k}(0)$ | $C_K^{\alpha^*,k^*}(0)$ | $C_K^{HZ}(0)$ | MC | C.I. length | $U_K^{N,\Delta K}(0)$ | L |
|-----|---------------------|-------------------------|---------------|----------|------------------------|-----------------------|-------|
| 0.0 | 8.792318 | 8.792318 | N.A. | 8.792318 | 2.384×10^{-9} | N.A. | N.A. |
| 0.4 | 8.561005 | 8.561005 | 8.561005 | 8.561005 | 8.856×10^{-8} | 8.585020 | 0.15 |
| 0.8 | 8.333472 | 8.333472 | 8.333472 | 8.333472 | 1.975×10^{-7} | 8.357510 | 0.05 |
| 1.2 | 8.109743 | 8.109743 | 8.109744 | 8.109744 | 7.078×10^{-7} | 8.133828 | -0.05 |
| 1.6 | 7.889839 | 7.889839 | 7.889840 | 7.889840 | 8.442×10^{-7} | 7.913947 | -0.15 |
| 2.0 | 7.673778 | 7.673778 | 7.673781 | 7.673781 | 1.366×10^{-6} | 7.697839 | -0.25 |
| 2.4 | 7.461575 | 7.461575 | 7.461579 | 7.461580 | 1.905×10^{-6} | 7.485589 | 0.15 |
| 2.8 | 7.253242 | 7.253242 | 7.253248 | 7.253247 | 1.690×10^{-6} | 7.277280 | 0.05 |
| 3.2 | 7.048788 | 7.048788 | 7.048796 | 7.048797 | 2.580×10^{-6} | 7.072873 | -0.05 |
| 3.6 | 6.848219 | 6.848219 | 6.848228 | 6.848227 | 2.717×10^{-6} | 6.872327 | -0.15 |
| 4.0 | 6.651536 | 6.651536 | 6.651548 | 6.651546 | 2.709×10^{-6} | 6.675598 | -0.25 |

Table 2: Prices of the spread option computed for strike K in the jump diffusion model I of subsection 6.2. The parameter values are $S_1(0) = 100$, $S_2(0) = 96$, $\delta_1 = 0.03$, $\delta_2 = 0.05$, $\sigma_1 = 0.15$, $\sigma_2 = 0.1$, $\rho = 0.5$, $r = 0.1$, $\lambda = 0.2$, $\alpha_1 = 0.06$, $\alpha_2 = 0.03$, $\xi_1 = 0.03$, $\xi_2 = 0.09$, $\rho_y = -0.8$, $\lambda_1 = 0.2$, $\alpha_{11} = 0.02$, $\xi_{11} = 0.06$, $\lambda_2 = 0.1$, $\alpha_{22} = -0.07$, $\xi_{22} = 0.01$, $M = 10^6$, $N = 1000$, and $\Delta K = 0.5$. Hurd and Zhou parameters are $N^{HZ} = 512$, $\bar{u} = 40$ and $\epsilon = [-3, 1]^T$. Column labels are as in Table 1.

| K | $C_K^{\alpha,k}(0)$ | $C_K^{\alpha^*,k^*}(0)$ | $C_K^{HZ}(0)$ | MC | C.I. length | $U_K^{N,\Delta K}(0)$ | L |
|-----|---------------------|-------------------------|---------------|----------|------------------------|-----------------------|-------|
| 0.0 | 8.815578 | 8.815578 | N.A. | 8.815578 | 2.019×10^{-8} | N.A. | N.A. |
| 0.4 | 8.585660 | 8.585660 | 8.585661 | 8.585661 | 8.677×10^{-8} | 8.622451 | 0.15 |
| 0.8 | 8.359561 | 8.359561 | 8.359561 | 8.359561 | 5.559×10^{-7} | 8.396375 | 0.05 |
| 1.2 | 8.137301 | 8.137301 | 8.137302 | 8.137303 | 1.989×10^{-6} | 8.174163 | -0.05 |
| 1.6 | 7.918901 | 7.918901 | 7.918903 | 7.918903 | 1.268×10^{-6} | 7.955786 | -0.15 |
| 2.0 | 7.704377 | 7.704377 | 7.704380 | 7.704381 | 1.862×10^{-6} | 7.741215 | -0.25 |
| 2.4 | 7.493741 | 7.493741 | 7.493746 | 7.493747 | 3.560×10^{-6} | 7.530532 | 0.15 |
| 2.8 | 7.287004 | 7.287004 | 7.287010 | 7.287011 | 2.913×10^{-6} | 7.323818 | 0.05 |
| 3.2 | 7.084171 | 7.084172 | 7.084180 | 7.084179 | 2.658×10^{-6} | 7.121033 | -0.05 |
| 3.6 | 6.885247 | 6.885247 | 6.885257 | 6.885257 | 3.056×10^{-6} | 6.922132 | -0.15 |
| 4.0 | 6.690231 | 6.690231 | 6.690244 | 6.690244 | 4.336×10^{-6} | 6.727069 | -0.25 |

Table 3: Prices of the spread option computed for strike K in the jump diffusion model II of subsection 6.3. The parameter values are $S_1(0) = 100$, $S_2(0) = 96$, $\delta_1 = 0.03$, $\delta_2 = 0.05$, $\sigma_1 = 0.15$, $\sigma_2 = 0.1$, $\rho = 0.5$, $r = 0.1$, $\lambda = 0.2$, $\alpha_1 = 0.06$, $\alpha_2 = 0.03$, $\xi_1 = 0.03$, $\xi_2 = 0.09$, $\rho_y = -0.8$, $\lambda_1 = 0.2$, $\alpha_{11} = 0.02$, $\xi_{11} = 0.06$, $\lambda_2 = 0.1$, $\alpha_{22} = -0.07$, $\xi_{22} = 0.01$, $M = 10^6$, $N = 1000$, and $\Delta K = 0.5$. Hurd and Zhou parameters are $N^{HZ} = 512$, $\bar{u} = 40$ and $\epsilon = [-3, 1]^T$. Column labels are as in Table 1.

| K | $C_K^{\alpha,k}(0)$ | $C_K^{\alpha^*,k^*}(0)$ | $C_K^{HZ}(0)$ | MC | C.I. length | $U_K^{N,\Delta K}(0)$ | L |
|-----|---------------------|-------------------------|---------------|----------|------------------------|-----------------------|-------|
| 0.0 | 3.863711 | 3.863711 | N.A. | 3.863711 | 2.373×10^{-8} | N.A. | N.A. |
| 2.0 | 2.230264 | 2.230267 | N.A. | 2.230270 | 8.027×10^{-7} | 2.295558 | -0.50 |
| 2.2 | 2.083929 | 2.083933 | N.A. | 2.083937 | 1.241×10^{-6} | 2.149442 | -0.30 |
| 2.4 | 1.942230 | 1.942235 | N.A. | 1.942240 | 1.162×10^{-6} | 2.007675 | -0.10 |
| 2.6 | 1.805556 | 1.805562 | N.A. | 1.805568 | 1.373×10^{-6} | 1.870806 | 0.10 |
| 2.8 | 1.674271 | 1.674278 | N.A. | 1.674285 | 1.949×10^{-6} | 1.739391 | 0.30 |
| 3.0 | 1.548706 | 1.548715 | N.A. | 1.548722 | 1.983×10^{-6} | 1.614000 | -0.50 |
| 3.2 | 1.429154 | 1.429164 | N.A. | 1.429172 | 1.826×10^{-6} | 1.494667 | -0.30 |
| 3.4 | 1.315855 | 1.315867 | N.A. | 1.315876 | 2.254×10^{-6} | 1.381300 | -0.10 |
| 3.6 | 1.208999 | 1.209012 | N.A. | 1.209022 | 2.112×10^{-6} | 1.274248 | 0.10 |
| 3.8 | 1.108713 | 1.108727 | N.A. | 1.108739 | 2.324×10^{-6} | 1.173832 | 0.30 |
| 4.0 | 1.015062 | 1.015077 | N.A. | 1.015089 | 2.723×10^{-6} | 1.080355 | -0.50 |

Table 4: Prices of the spread option computed for strike K in the mean-reverting jump diffusion model of subsection 6.4. The parameter values are $f_1(T) = \ln(30)$, $f_2(T) = \ln(26)$, $X_1(0) = 0$, $X_2(0) = 0$, $Y_1(0) = 0$, $Y_2(0) = 0$, $\sigma_1 = 0.1$, $\sigma_2 = 0.08$, $\rho = 0.5$, $r = 0.1$, $\alpha_1 = 0.6$, $\alpha_2 = 0.6$, $\lambda_1^+ = 0.025$, $\lambda_1^- = 0.02$, $\lambda_2^+ = 0.03$, $\lambda_2^- = 0.025$, $\mu_1^+ = 0.3$, $\mu_1^- = 0.35$, $\mu_2^+ = 0.3$, $\mu_2^- = 0.37$, $M = 10^6$, $N = 1500$, and $\Delta K = 1$. Column labels are as in Table 1.

| K | $C_K^{\alpha,k}(0)$ | $C_K^{\alpha^*,k^*}(0)$ | $C_K^{HZ}(0)$ | MC | C.I. length | $U_K^{N,\Delta K}(0)$ | L |
|-----|---------------------|-------------------------|---------------|----------|------------------------|-----------------------|-------|
| 0.0 | 8.542801 | 8.542801 | N.A. | 8.542802 | 1.684×10^{-7} | N.A. | N.A. |
| 2.0 | 7.548500 | 7.548500 | 7.548502 | 7.548502 | 8.730×10^{-7} | 7.565996 | -0.25 |
| 2.2 | 7.453534 | 7.453534 | 7.453536 | 7.453537 | 1.133×10^{-6} | 7.471050 | -0.05 |
| 2.4 | 7.359379 | 7.359379 | 7.359381 | 7.359382 | 1.275×10^{-6} | 7.376834 | 0.15 |
| 2.6 | 7.266033 | 7.266033 | 7.266037 | 7.266037 | 1.451×10^{-6} | 7.283569 | -0.15 |
| 2.8 | 7.173498 | 7.173498 | 7.173501 | 7.173501 | 1.561×10^{-6} | 7.190973 | 0.05 |
| 3.0 | 7.081771 | 7.081771 | 7.081775 | 7.081775 | 1.447×10^{-6} | 7.099266 | -0.25 |
| 3.2 | 6.990852 | 6.990852 | 6.990857 | 6.990857 | 2.095×10^{-6} | 7.008368 | -0.05 |
| 3.4 | 6.900740 | 6.900740 | 6.900745 | 6.900745 | 1.995×10^{-6} | 6.918195 | 0.15 |
| 3.6 | 6.811434 | 6.811434 | 6.811440 | 6.811440 | 2.281×10^{-6} | 6.828970 | -0.15 |
| 3.8 | 6.722932 | 6.722932 | 6.722939 | 6.722939 | 2.099×10^{-6} | 6.740408 | 0.05 |
| 4.0 | 6.635234 | 6.635234 | 6.635242 | 6.635241 | 2.214×10^{-6} | 6.652730 | -0.25 |

Table 5: Prices of the spread option computed for strike K in the three-factor stochastic volatility model of subsection 6.5. The parameter values are $S_1(0) = 100$, $S_2(0) = 96$, $\rho = 0.5$, $\sigma_1 = 1.0$, $\sigma_2 = 0.5$, $\rho_1 = -0.5$, $\rho_2 = 0.25$, $\delta_1 = 0.05$, $\delta_2 = 0.05$, $v_0 = 0.04$, $\kappa = 1.0$, $\mu = 0.04$, $\sigma_v = 0.05$, $r = 0.1$, $T = 1.0$. $M = 10^6$, $N = 1000$, and $\Delta K = 0.5$. Hurd and Zhou parameters are $N^{HZ} = 512$, $\bar{u} = 40$ and $\epsilon = [-3, 1]^T$. Column labels are as in Table 1.

| K | $C_K^{\alpha,k}(0)$ | $C_K^{\alpha^*,k^*}(0)$ | $C_K^{HZ}(0)$ | MC | C.I. length | $U_K^{N,\Delta K}(0)$ | L |
|-----|---------------------|-------------------------|---------------|-----------|------------------------|-----------------------|-------|
| 0.0 | 10.737350 | 10.737350 | N.A. | 10.737351 | 3.873×10^{-8} | N.A. | N.A. |
| 2.0 | 9.727443 | 9.727444 | 9.727458 | 9.727458 | 1.385×10^{-6} | 9.913266 | -0.25 |
| 2.2 | 9.629988 | 9.629990 | 9.630006 | 9.630006 | 1.558×10^{-6} | 9.815825 | -0.05 |
| 2.4 | 9.533178 | 9.533180 | 9.533200 | 9.533200 | 1.811×10^{-6} | 9.718963 | 0.15 |
| 2.6 | 9.437015 | 9.437017 | 9.437040 | 9.437040 | 2.005×10^{-6} | 9.622871 | -0.15 |
| 2.8 | 9.341499 | 9.341501 | 9.341528 | 9.341527 | 2.240×10^{-6} | 9.527299 | 0.05 |
| 3.0 | 9.246629 | 9.246632 | 9.246662 | 9.246664 | 2.575×10^{-6} | 9.432452 | -0.25 |
| 3.2 | 9.152407 | 9.152410 | 9.152445 | 9.152445 | 2.638×10^{-6} | 9.338245 | -0.05 |
| 3.4 | 9.058833 | 9.058837 | 9.058875 | 9.058876 | 2.924×10^{-6} | 9.244618 | 0.15 |
| 3.6 | 8.965907 | 8.965911 | 8.965954 | 8.965955 | 3.262×10^{-6} | 9.151762 | -0.15 |
| 3.8 | 8.873628 | 8.873633 | 8.873681 | 8.873681 | 3.535×10^{-6} | 9.059429 | 0.05 |
| 4.0 | 8.781998 | 8.782003 | 8.782057 | 8.782057 | 3.735×10^{-6} | 8.967821 | -0.25 |

Table 6: Prices of the spread option computed for strike K in the VG mixture model of subsection 6.6. The parameter values are $S_1(0) = 100$, $S_2(0) = 96$, $\rho = 0.5$, $a_+ = 20.4499$, $a_- = 24.4499$, $\alpha = 0.4$, $\lambda = 10$, $r = 0.1$, $T = 1.0$. $M = 10^7$, $N = 1000$, and $\Delta K = 0.5$. Hurd and Zhou parameters are $N^{HZ} = 512$, $\bar{u} = 40$ and $\epsilon = [-3, 1]^T$. Column labels are as in Table 1.

| K | $C_K^{\alpha,k}(0)$ | $C_K^{\alpha^*,k^*}(0)$ | $C_K^{HZ}(0)$ | MC | C.I. length | $U_K^{N,\Delta K}(0)$ | L |
|-----|---------------------|-------------------------|---------------|----------|------------------------|-----------------------|-------|
| 0.0 | 6.292223 | 6.292223 | N.A. | 6.292224 | 1.222×10^{-7} | N.A. | N.A. |
| 2.0 | 4.946084 | 4.946121 | 4.946198 | 4.946192 | 1.697×10^{-5} | 5.159785 | -0.25 |
| 2.2 | 4.818943 | 4.818990 | 4.819082 | 4.819087 | 2.051×10^{-5} | 5.032506 | -0.05 |
| 2.4 | 4.693307 | 4.693365 | 4.693474 | 4.693483 | 2.481×10^{-5} | 4.906937 | 0.15 |
| 2.6 | 4.569215 | 4.569286 | 4.569415 | 4.569428 | 2.852×10^{-5} | 4.782801 | -0.15 |
| 2.8 | 4.446705 | 4.446791 | 4.446946 | 4.446950 | 2.977×10^{-5} | 4.659357 | 0.05 |
| 3.0 | 4.325819 | 4.325922 | 4.326108 | 4.326106 | 3.317×10^{-5} | 4.539521 | -0.25 |
| 3.2 | 4.206597 | 4.206720 | 4.206943 | 4.206952 | 3.922×10^{-5} | 4.420160 | -0.05 |
| 3.4 | 4.089081 | 4.089225 | 4.089492 | 4.089508 | 4.530×10^{-5} | 4.302711 | 0.15 |
| 3.6 | 3.973312 | 3.973481 | 3.973796 | 3.973802 | 5.102×10^{-5} | 4.186898 | -0.15 |
| 3.8 | 3.859334 | 3.859530 | 3.859897 | 3.859885 | 5.517×10^{-5} | 4.071985 | 0.05 |
| 4.0 | 3.747190 | 3.747416 | 3.747838 | 3.747834 | 6.101×10^{-5} | 3.960891 | -0.25 |

Table 7: Prices of the spread option computed for strike K in the VG time changed model of subsection 6.7. The parameter values are $S_1(0) = 51$, $S_2(0) = 47$, $M = 10^6$, $T = 1.0$, $v(0) = 1.0$, $r = 0.1$, $a_1 = 0.5971$, $a_2 = 0.7801$, $\sigma_1 = 0.2824$, $\sigma_2 = 0.1849$, $\sigma_Z = 0.3497$, $\delta_1 = 0.018$, $\delta_2 = 0.03$, $v_1 = 0.1726$, $v_2 = 2.2360$, $v_Z = 0.2$, $\theta_1 = -0.1144$, $\theta_2 = 0.0962$, $\theta_Z = -1.0417$, $\lambda = 0.8332$, $k = 1.0992$, $\eta = 1.1275$, $b_1 = 0.2219$, $b_2 = 0.2351$, $N = 1000$, and $\Delta K = 0.5$. Hurd and Zhou parameters are $N^{HZ} = 1024$, $\bar{u} = 160$ and $\epsilon = [-3, 1]^T$. Column labels are as in Table 1.

| Model | $C_K^{\alpha,k}(0)$ | $C_K^{HZ}(0)$ |
|--------------------------------|---------------------|---------------|
| Geometric Brownian motion | 0.004440 | 0.655636 |
| Jump diffusion I | 0.003709 | 0.713311 |
| Jump diffusion II | 0.004350 | 0.740647 |
| Mean-reverting jump diffusion | 0.005154 | N.A. |
| 3-factor stochastic volatility | 0.006818 | 0.898995 |
| VG mixture | 0.006341 | 0.876933 |
| VG time changed | 0.037638 | 6.021662 |

Table 8: The Gauss–Kronrod quadrature rule in $C_K^{\alpha,k}(0)$ and the bivariate Fourier inversion in $C_K^{HZ}(0)$ are compared in terms of computational cost. The computing times for the spread option value are given for each model. The simulation settings and the model parameters are set as in Tables 1 to 7. The option strike price is always $K = 2$.

| | $\Delta(S_1(0))$ | $\Delta(S_2(0))$ | $\Theta(T)$ | $\text{Vega}(\sigma_1)$ | $\text{Vega}(\sigma_2)$ | $\text{Rho}(\rho)$ |
|---------------------|------------------|------------------|-------------|-------------------------|-------------------------|--------------------|
| $C_K^{\alpha,k}(0)$ | 0.512705 | -0.447078 | 3.023768 | 33.114873 | -0.799270 | -4.193731 |
| $C_K^{HZ}(0)$ | 0.512705 | -0.447079 | 3.023777 | 33.114834 | -0.798972 | -4.193728 |

Table 9: The Greeks for the GBM model compared between the lower bound $C_K^{\alpha,k}(0)$ and the Hurd and Zhou (2010) solution $C_K^{HZ}(0)$. The Greeks for $C_K^{HZ}(0)$ use $N = 2^{10}$ and $\bar{u} = 40$. Model parameters are as in Table 1 and the strike price is set to $K = 4$.

| Model | MC | C.I. length | MC ^{cr} | C.I. length ^{cr} |
|--------------------------------|----------|------------------------|------------------|---------------------------|
| Geometric Brownian motion | 7.542324 | 3.088×10^{-7} | 7.547870 | 1.415×10^{-2} |
| Jump diffusion I | 7.673781 | 1.366×10^{-6} | 7.684104 | 4.013×10^{-2} |
| Jump diffusion II | 7.704381 | 1.862×10^{-6} | 7.693970 | 4.149×10^{-2} |
| Mean-reverting jump diffusion | 2.230270 | 8.027×10^{-7} | 2.231747 | 1.149×10^{-2} |
| 3-factor stochastic volatility | 7.548502 | 8.730×10^{-7} | 7.577023 | 4.297×10^{-2} |
| VG mixture | 9.727458 | 1.385×10^{-6} | 9.722541 | 1.744×10^{-2} |
| VG time changed | 4.946192 | 1.697×10^{-5} | 4.929361 | 2.219×10^{-2} |

Table 10: The control variate (MC) and the crude (MC^{cr}) Monte Carlo are compared for each model. The simulation settings and the model parameters are set as in Tables 1 to 7. The option strike price is always $K = 2$. The confidence interval length of the Monte Carlo simulation is also provided.